The Dynamics of a Roll Press Nip

**Problem presented by John Skelton,
Albany International**

15th Annual Workshop on Mathematical Problems in Industry, University of Delaware, Newark, DE USA June 7-11 1999

1 Introduction

The problem presented at the workshop by John Skelton of Albany International concerned the dynamics of a roll press nip, a crucial component in a paper-making machine. Modern commercial paper-making machines are huge items of equipment. They may be as long as a football field and cost many millions of dollars each. Integrity of the process is extremely important; the paper in such a machine travels so fast (up to 20 km/sec) that a break is viewed as a major calamity and may take many man-hours and dollars to recover from. The size and speed of the machines means that it is not easy to make measurements as the paper passes through. The hostility of the environment therefore dictates that a thorough theoretical understanding of the important parts of the process is crucial if the processes involved are to be optimized.

A modern paper-making machine is divided into three sections: a forming section, a pressing section and a drying section. In the forming section, raw materials are combined to form a wet paper mixture. The priority is now to remove the maximum possible amount of water without affecting the structural integrity of the paper. Most of the required water removal is accomplished in the pressing section, and it is this part of the machine that we wish specifically to study. The key requirement of the press section is that water removal should be via mechanical means, for though thermal drying is employed at later stages (in the drying section) in the paper-making process, it is much more expensive than a simple squeezing process when the water content of the paper is high.

The basic mechanical means by which the press section of a paper-making machine functions involves the process of squeezing the paper between two rollers. This happens many times and in many different ways to a single portion of the paper sheet; we shall examine a single pass through such a "Roll press nip". A great deal of water is removed by this process; typically on first entry into the roll press nip the paper consists of 20% fiber and 80% water whilst on exit from this part of the paper making machine the water content has been reduced to 60%. The remaining water is then removed by the drying section of the machine, after which it comprises roughly 5% water.

A schematic diagram of a typical roll press nip is shown in figure 1. The two steel rollers are typically each about 1m in diameter. The just-formed paper (typically about 0.5mm thick) enters the roll press nip seated on a fabric sheet (hereinafter referred to as "felt"). The felt is a fabric that is composed of nylon textile fibers (typical diameter 20μ); it may be regarded as a porous medium that, in its undeformed state, is about 3mm thick. Before deformation under the rollers, the felt has a solid volume fraction of about 50%; during loading, this may increase to 80%. As the paper sheet and fabric enter the nip region, both are compressed. During compression the fabric structure deforms and the water is squeezed out of the paper and the fabric. Although a number of different arrangements are possible, the water usually passes into the bottom roller via holes or slots. We therefore assume that, once the water has been squeezed out of the paper and the fabric, it disappears. After the squeezing has taken place, the felt is removed by the bottom roller, whilst the paper remains in contact with the top roller for a little longer; the paper is then wound on to a smaller paper roller. In this way the felt travels in a closed loop. A typical feed speed is about 20m/s and the pressure under the rollers may reach 10MPa. Of course, a roll press is a very complicated item of equipment and we have only been able to indicate its main features; the interested reader may find more details in Reese (1999).

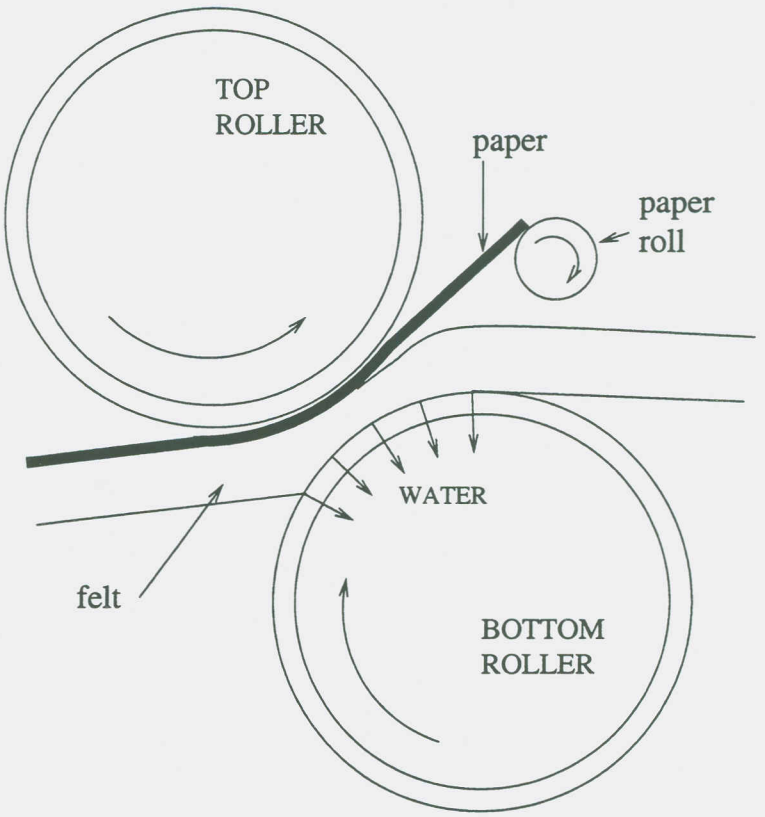

Figure 1: Schematic diagram of typical roll press nip

1.1 Problem Objectives

In this study we do not seek to answer any one specific question, but rather wish to propose a general framework for modeling the flow and deformation under a roll press nip. Because of the difficulty of making measurements in the nip region and the need to closely control the process, the distributions of pressure, velocity and felt porosity within the nip have traditionally been subjects of great debate.

Previous treatments have included lubrication theory models and "Bernoulli" based models. Although some progress may be made using thin layer theory, we shall show the required modeling does not take the form of standard lubrication theory. As far as models based on Bernoulli's equation are concerned, we simply note that the discussion below shows that the drag force exerted by the felt on the liquid is a key physical component of the flow process. Clearly, a full three-phase flow treatment is required. In this study we will thus address the following questions:

(i) Is it possible to propose a general theoretical treatment of the roll press nip?

(ii) What determines the physics of the water movement within the paper and felt in the roll press nip and how is this connected to the details of the air movement and the deformation of the felt?

(iii) When a general model has been proposed, is it possible exploit the geometry within the nip to generate some simple exact solutions?

(iv) What are the key non-dimensional parameters in the problem and how large are they likely to be for realistic paper-making machines?

A further matter of interest concerns the influence that the size, shape and separation of the rollers have on the whole process.

We approach the modeling from a rather general point of view, beginning by including all effects that might be important and then making clearly defined assumptions to simplify the equations. In this way it is possible to make changes to the model if circumstances change.

2 Three phase flow modeling

A general roll press nip consists of two materials, namely paper and felt, each of which may contain either water, air, or water and air. The water and air may flow and the paper or felt may compress or expand; it is therefore necessary to treat the problem as a three-phase flow model. We do not distinguish henceforth between paper and felt, regarding the paper as being essentially the same as felt, save for the fact that the material properties are different. The three phases that will be considered are therefore water, air and felt.

We assume that both the water and the air are incompressible, so that any flow that takes place does so with a constant density; the compressibility of the water is certainly negligible and though compressible effects concerned with the flow of the air could be included if required it seems highly unlikely that they will be important. They are thus henceforth ignored. Since the rollers are also extremely long, we shall also ignore end effects and consider only a two dimensional model of the process (though the equations that we propose are completely general and thus applicable to three dimensions) with position vector given by $\boldsymbol{x} = (x, z)^T$. Since we wish to propose a model that combines both flow and elasticity, notation is something of a problem; after some consideration we finally decided to denote the water (liquid), air and felt velocities by $\boldsymbol{q}_\ell = (u_\ell, w_\ell)^T$, $\boldsymbol{q}_a = (u_a, w_a)^T$ and $\boldsymbol{q}_f = (u_f, w_f)^T$ respectively and the felt displacements by $\boldsymbol{U} = (U, W)^T$. Before the rollers (and any upstream influence that they might generate) are encountered, we assume that the air and water filled felt moves with a speed $u_\infty \sim 20$m/s and thus $\boldsymbol{q}_\ell = \boldsymbol{q}_a = \boldsymbol{q}_f = (u_\infty, 0)^T$, and also that $\boldsymbol{U} = (u_\infty t, 0)^T$ and the void fractions of liquid and air in the felt are known. A schematic diagram of

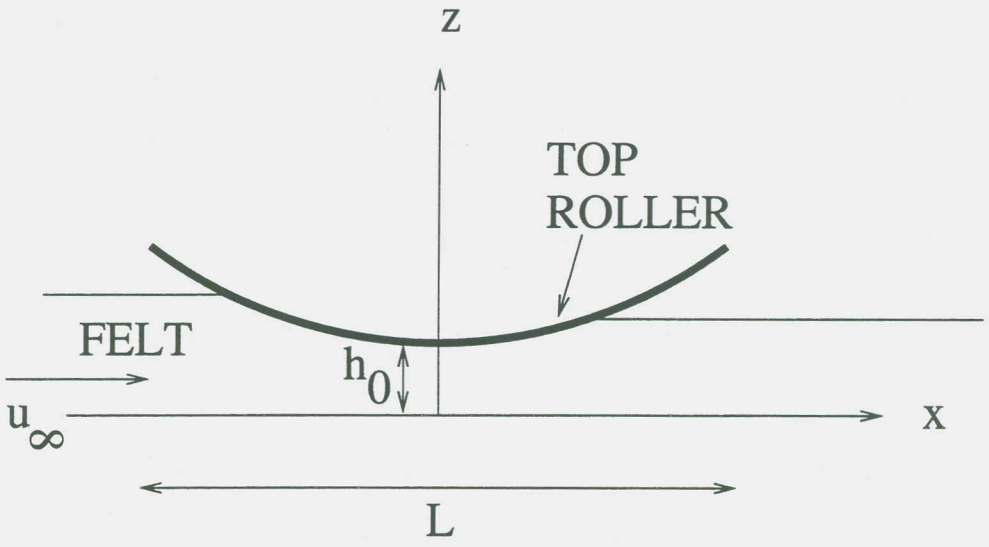

Figure 2: Schematic diagram of flow under a roll press nip

the flow region is shown in figure 2. The region under which the influence of the rollers is perceived and water is squeezed out of the felt is assumed to have length $L \sim 0.02$m, and a typical distance between rollers is denoted by $h_0 \sim 0.002$m. We denote a typical pore size in the felt by $a \sim 10^{-5}$m.

We begin with a rather general form of the three phase flow mass and momentum conservation equations for the liquid, air and felt respectively (for a derivation see, for example, Drew & Wood (1985)): these are

$$(\rho_\ell \alpha)_t + \nabla.(\rho_\ell \alpha \boldsymbol{q}_\ell) = 0 \quad (1)$$

$$(\rho_a \beta)_t + \nabla.(\rho_a \beta \boldsymbol{q}_a) = 0 \quad (2)$$

$$(\rho_f (1-\alpha-\beta))_t + \nabla.(\rho_f (1-\alpha-\beta)\boldsymbol{q}_f) = 0 \quad (3)$$

$$(\rho_\ell \alpha \boldsymbol{q}_\ell)_t + \nabla.(\rho_\ell \alpha \boldsymbol{q}_\ell \boldsymbol{q}_\ell) = \nabla.(\alpha(\boldsymbol{T}_\ell + \boldsymbol{T}_\ell^{Re})) + \alpha\rho_\ell \boldsymbol{b} + \boldsymbol{M}_\ell \quad (4)$$

$$(\rho_a \beta \boldsymbol{q}_a)_t + \nabla.(\rho_a \beta \boldsymbol{q}_a \boldsymbol{q}_a) = \nabla.(\beta(\boldsymbol{T}_a + \boldsymbol{T}_a^{Re})) + \beta\rho_a \boldsymbol{b} + \boldsymbol{M}_a \quad (5)$$

$$(\rho_f (1-\alpha-\beta)\boldsymbol{q}_f)_t + \nabla.(\rho_f (1-\alpha-\beta)\boldsymbol{q}_f \boldsymbol{q}_f) = \nabla.((1-\alpha-\beta)(\boldsymbol{T}_f + \boldsymbol{T}_f^{Re})) + (1-\alpha-\beta)\rho_f \boldsymbol{b} + \boldsymbol{M}_f. \quad (6)$$

Here the densities of the liquid, air and water are denoted by ρ_ℓ, ρ_a and ρ_f respectively. The volume fraction of liquid is denoted by α and the fraction of air by β, and $\boldsymbol{b}$ denotes the applied body force. The stress tensors of the liquid, air and water are denoted by $\boldsymbol{T}_\ell$, $\boldsymbol{T}_a$ and $\boldsymbol{T}_f$ respectively, whilst the corresponding stress tensors arising from Reynolds stresses are denoted by $\boldsymbol{T}_\ell^{Re}$, $\boldsymbol{T}_a^{Re}$ and $\boldsymbol{T}_f^{Re}$. The $\boldsymbol{M}_i$ ($i = \ell, a$ or f) denote the interfacial momentum source terms.

It is important to remember that (1)–(6) (which have become the recognized starting point for models of many different multiphase flow regimes) are posed entirely in terms of *ensemble averaged* variables, the ensemble average $< f >$ of a field $f(\boldsymbol{x}, t)$ being defined by

$$< f > = \int_M f(\boldsymbol{x}, t; \zeta) d\mu(\zeta),$$

where $\mu(\zeta)$ is the probability of observing the result ζ and M the set of all such results. Space does not permit a discussion of the effects of averaging on the equations, but it is worth noting that (a) The $\boldsymbol{M}_i$ terms are a direct result of the averaging process and (b) that all profile coefficients (terms arising from the fact that the product of the average is not equal to the average of the product) have been set to unity.

It is now necessary to make some assumptions to proceed. It has become normal (see, for example Drew & Wood (1985)) to write

$$\boldsymbol{M}_\ell = p_{\ell i}\nabla\alpha + \boldsymbol{M}'_\ell$$

(with similar definitions for $\boldsymbol{M}_a$ and $\boldsymbol{M}_f$), where p_{ki} is the average interfacial pressure of phase k and the terms $\boldsymbol{M}'_k$ contain all forces that are related to drag, virtual mass, Bassett and Faxen forces and any other unsteady flow effects that might be important. In this case, we ignore all such effects except for the interphase drag forces and denote the drag force per unit volume on phase i due to phase j by

$\boldsymbol{D}_{ij}$. Additionally, we assume that since the liquid and air flows through a porous medium, the flow is laminar and so there are no Reynolds stress terms. Given that we will later propose models for the drag forces, we assume that this accounts for all the important effects of viscosity, and thus in the liquid and air phases the stress tensors are given by $\boldsymbol{T}_\ell = -p_\ell \boldsymbol{I}$ and $\boldsymbol{T}_a = -p_a \boldsymbol{I}$ respectively. (Here and henceforth we use bold face for both vectors and tensors; the context should ensure that this results in no confusion.) We also assume that the only body force that may be important is gravity, For convenience, we also write $\gamma = 1 - \alpha - \beta$. The equations thus become

$$\begin{aligned}
(\rho_\ell\alpha)_t + \nabla.(\rho_\ell\alpha\boldsymbol{q}_\ell) &= 0 && (7)\\
(\rho_a\beta)_t + \nabla.(\rho_a\beta\boldsymbol{q}_a) &= 0 && (8)\\
(\rho_f\gamma)_t + \nabla.(\rho_f\gamma\boldsymbol{q}_f) &= 0 && (9)\\
(\rho_\ell\alpha\boldsymbol{q}_\ell)_t + \nabla.(\rho_\ell\alpha\boldsymbol{q}_\ell\boldsymbol{q}_\ell) &= -\nabla(\alpha p_\ell) + p_{\ell i}\nabla\alpha + \alpha\rho_\ell\boldsymbol{g} + \boldsymbol{D}_{\ell a} + \boldsymbol{D}_{\ell f} && (10)\\
(\rho_a\beta\boldsymbol{q}_a)_t + \nabla.(\rho_a\beta\boldsymbol{q}_a\boldsymbol{q}_a) &= -\nabla(\beta p_a) + p_{ai}\nabla\beta + \beta\rho_a\boldsymbol{g} + \boldsymbol{D}_{a\ell} + \boldsymbol{D}_{af} && (11)\\
(\rho_f\gamma\boldsymbol{q}_f)_t + \nabla.(\rho_f\gamma\boldsymbol{q}_f\boldsymbol{q}_f) &= \nabla.(\gamma\boldsymbol{T}_f) + p_{fi}\nabla\gamma + \gamma\rho_f\boldsymbol{g} + \boldsymbol{D}_{f\ell} + \boldsymbol{D}_{fa} && (12)
\end{aligned}$$

The equations (7)-(12) may be regarded as "general" equations for the roll press nip, but cannot be used in their present form; even if we assume that the drag forces are all known and the felt stress tensor is known in terms of the felt displacement, the system (thought of in three space dimensions) comprises $3 + 9 = 12$ equations in the 20 unknowns $\boldsymbol{q}_\ell$, $\boldsymbol{q}_a$, $\boldsymbol{q}_f$, $\boldsymbol{U}$, p_ℓ, p_a, p_f, $p_{\ell i}$, p_{ai}, p_{fi}, α and β. We must now therefore introduce some further simplifying assumptions into (7)–(12). First, Newton's third law implies that the relevant drag forces are equal and opposite so that

$$\boldsymbol{D}_{ij} = -\boldsymbol{D}_{ji}$$

for $i, j = \ell$, a or f.

Next, we consider the relationship between the bulk and interfacial pressures. For simplicity we shall assume here that the bulk pressure in each phase is equal the interfacial pressure. Of course, this assumption is evidently false. For inviscid flow around a sphere, for example, it is clear that the fluid pressure far from the sphere must be different from the pressure on the surface of the sphere; such phenomena are usually referred to as "Bernoulli effects". In this scenario, however, we expect that the errors introduced by the neglect of Bernoulli effects (which could be included in a fairly simple manner if desired) will be small. Additionally, we observe that it will transpire that the inertia terms in the equations are small and may be ignored. Though it is well-established that the neglect of Bernoulli effects may lead to serious errors (including change-of-type difficulties; see for example Fitt (1996)) when inertia is important, no such problems arise for inertia-free multiphase flow.

A further assumption will now be made concerning the pressures - it will be assumed that the phasic bulk pressures are equal so that $p_\ell = p_a = p_f = p$. This assumption is tantamount to ignoring any surface energy effects (and these could easily be incorporated into the model if desired).

Finally, we assume that the stress tensor $\boldsymbol{T}_f$ in the felt may be written as

$$\gamma\boldsymbol{T}_f = -\gamma p_f \boldsymbol{I} + \boldsymbol{\tau}_f\,,$$

where the felt deviatoric stress tensor $\boldsymbol{\tau}_f$ accounts for effects not due to pressures (i.e. those due to elastic deformations). (We note that since by convention $p > 0$ is taken to signify compression, the

presence of the terms $-\gamma p$ and $\boldsymbol{\tau}_f$ in the above formulation of $\boldsymbol{T}_f$ implies that $\tau_{f22} > 0$ corresponds to a state of positive tension.) This gives the "working equations"

$$\begin{aligned}
\alpha_t + \nabla.(\alpha \boldsymbol{q}_\ell) &= 0 && (13)\\
\beta_t + \nabla.(\beta \boldsymbol{q}_a) &= 0 && (14)\\
\gamma_t + \nabla.(\gamma \boldsymbol{q}_f) &= 0 && (15)\\
(\rho_\ell \alpha \boldsymbol{q}_\ell)_t + \nabla.(\rho_\ell \alpha \boldsymbol{q}_\ell \boldsymbol{q}_\ell) &= -\alpha \nabla p + \alpha \rho_\ell \boldsymbol{g} + \boldsymbol{D}_{\ell a} + \boldsymbol{D}_{\ell f} && (16)\\
(\rho_a \beta \boldsymbol{q}_a)_t + \nabla.(\rho_a \beta \boldsymbol{q}_a \boldsymbol{q}_a) &= -\beta \nabla p + \beta \rho_a \boldsymbol{g} - \boldsymbol{D}_{\ell a} + \boldsymbol{D}_{af} && (17)\\
(\rho_f \gamma \boldsymbol{q}_f)_t + \nabla.(\rho_f \gamma \boldsymbol{q}_f \boldsymbol{q}_f) &= -\gamma \nabla p + \nabla.\boldsymbol{\tau}_f + \gamma \rho_f \boldsymbol{g} - \boldsymbol{D}_{\ell f} - \boldsymbol{D}_{af} && (18)
\end{aligned}$$

2.1 Dimensional Analysis

Non-dimensionalisation of (13)–(18) may now take place. We scale according to $\boldsymbol{x} = L\boldsymbol{x}^*$, $t = (L/u_\infty)t^*$, $\boldsymbol{q}_i = u_\infty \boldsymbol{q}_i^*$ (for $i = \ell$, a or f), $\boldsymbol{U} = L\boldsymbol{U}^*$, $p = Ep^*$, $\boldsymbol{D}_{ij} = (E/L)\boldsymbol{D}_{ij}^*$ (for $i, j = \ell$, a or f) and $\boldsymbol{\tau}_f = E\boldsymbol{\tau}_f^*$ where the stars (which will henceforth be dropped) indicate non-dimensional variables and E is Young's modulus ($= \mu(3\lambda + 2\mu)/(\lambda + \mu)$ in terms of the Lamé constants). Some comment is appropriate concerning the choice of length scale: both of the other two important length scales in the problem (a and h_0) are much smaller than L, so for this initial consideration of the sizes of various terms in the equations we scale using L. Later, when we want to take advantage of the fact that $h_0/L \ll 1$, it will be appropriate to rescale accordingly. Rearranging, we find that the non-dimensional equations are

$$\begin{aligned}
\alpha_t + \nabla.(\alpha \boldsymbol{q}_\ell) &= 0\\
\beta_t + \nabla.(\beta \boldsymbol{q}_a) &= 0\\
\gamma_t + \nabla.(\gamma \boldsymbol{q}_f) &= 0\\
\Theta_\ell[(\alpha \boldsymbol{q}_\ell)_t + \nabla.(\alpha \boldsymbol{q}_\ell \boldsymbol{q}_\ell)] &= -\alpha \nabla p - \Lambda_\ell \alpha \boldsymbol{e}_z + \boldsymbol{D}_{\ell a} + \boldsymbol{D}_{\ell f}\\
\Theta_a[(\beta \boldsymbol{q}_a)_t + \nabla.(\beta \boldsymbol{q}_a \boldsymbol{q}_a)] &= -\beta \nabla p - \Lambda_a \beta \boldsymbol{e}_z - \boldsymbol{D}_{\ell a} + \boldsymbol{D}_{af}\\
\Theta_f[(\gamma \boldsymbol{q}_f)_t + \nabla.(\gamma \boldsymbol{q}_f \boldsymbol{q}_f)] &= -\gamma \nabla p + \nabla.\boldsymbol{\tau}_f - \Lambda_f \gamma \boldsymbol{e}_z - \boldsymbol{D}_{\ell f} - \boldsymbol{D}_{af}
\end{aligned}$$

where $\boldsymbol{e}_z$ is a unit vector in the z-direction and the non-dimensional parameters Θ_i and Λ_i are defined by

$$\Theta_i = \frac{\rho_i u_\infty^2}{E}, \qquad \Lambda_i = \frac{L\rho_i g}{E}$$

for $i = \ell, a$ or f. Since $u_\infty \sim 20\text{m/s}$, $L \sim 0.02\text{m}$, $E \sim 10^7\text{Pa}$, $\rho_f \sim \rho_\ell \sim 10^3\text{kg/m}^3$ and $\rho_a \sim 1\text{kg/m}^3$, none of the Θ_i exceeds 4×10^{-2} and none of the Λ_i exceeds 2×10^{-5}. Thus the effects of both inertia and gravity may be ignored. We also assume at this point that the only drag force that is important is the drag force between the liquid and the felt; once again other drag forces could be included as required. Thus $\boldsymbol{D}_{\ell a} = \boldsymbol{D}_{af} = 0$ and we obtain the non-dimensional equations

$$\begin{aligned}
\alpha_t + \nabla.(\alpha \boldsymbol{q}_\ell) &= 0 && (19)\\
\beta_t + \nabla.(\beta \boldsymbol{q}_a) &= 0 && (20)\\
\gamma_t + \nabla.(\gamma \boldsymbol{q}_f) &= 0 && (21)\\
0 &= -\alpha \nabla p + \boldsymbol{D}_{\ell f} && (22)\\
0 &= -\beta \nabla p && (23)\\
0 &= -\gamma \nabla p + \nabla.\boldsymbol{\tau}_f - \boldsymbol{D}_{\ell f} && (24)
\end{aligned}$$

These equations apply to either saturated or unsaturated regimes of flow, for from (23) we see that in the former case we have $\beta = 0$ and $\nabla p \neq 0$, whilst in the latter $\beta > 0$ and $\nabla p = 0$.

2.2 Constitutive Assumptions

In order to close (19)-(24) it is now necessary to make a number of constitutive assumptions. We attend to each assumption in turn:

2.2.1 DRAG:

For the drag $\boldsymbol{D}_{\ell f}$ exerted on the liquid phase by the felt we assume that Ergun's law applies so that (in dimensional variables)

$$\boldsymbol{D}_{\ell f} = -\frac{\mu_\ell \alpha}{a^2 k(\alpha)}(\boldsymbol{q}_\ell - \boldsymbol{q}_f) g(Re_p, \alpha), \tag{25}$$

where g is dimensionless, the pore scale Reynolds number Re_p is defined by

$$Re_p = \frac{a\rho_\ell \mid \boldsymbol{q}_\ell - \boldsymbol{q}_f \mid}{\mu_\ell}$$

and $k(\alpha)$ is a dimensionless permeability. In non-dimensional variables we therefore have

$$\boldsymbol{D}^*_{\ell f} = -K\frac{\alpha}{k(\alpha)}(\boldsymbol{q}^*_\ell - \boldsymbol{q}^*_f) g(Re_p, \alpha), \tag{26}$$

where

$$K = \frac{L u_\infty \mu_\ell}{E a^2}.$$

To understand the rationale behind (25) and (26) it is best to return to Ergun's original paper (Ergun, 1952). Ergun considered flow through packed granular beds under gravity, finding that the pressure drop across the bed was due to a combination of what he called "kinetic" and "viscous" energy losses. For a bed of height L_b composed of particles with an effective diameter D_p, he found (based on experimental correlations and dimensional analysis) that, for a very wide range of conditions, the pressure drop $\triangle \mathcal{P}$ was given by

$$\frac{g \triangle \mathcal{P}}{L_b} = 150\frac{(1-\phi)^2}{\phi^3}\frac{\mu_\ell u_\ell}{D_p^2} + 1.75\,\frac{1-\phi}{\phi^3}\frac{\rho_\ell u_\ell^2}{D_p}, \tag{27}$$

where ϕ denotes the fractional void volume in the packed bed and μ_ℓ the dynamic viscosity of the liquid. It should be noted that here, in accordance with custom, Ergun measured the pressure drop $\triangle \mathcal{P}$ in units of pressure/g ("hydraulic head"). The pressure drop formula (27) has become accepted as being a good model for the drag through many different types of bed, including porous media. The first term in (27) may be interpreted as a "Darcy" term, (more important when the flow speed and the permeability are low) and the second (the kinetic term) as a pressure loss that is more important when the flow speed is higher. Of course, a general interpretation of (27) requires that (a) relative velocities are used and (b) the second term is changed to $\boldsymbol{u}_\ell \mid \boldsymbol{u}_\ell \mid$ to take account of multidirectional flow. In terms of our pressure p (i.e. measured in units of force/unit area) we thus have

$$\frac{\triangle p}{L} = 150\frac{(1-\phi)^2}{\phi^3}\frac{\mu_\ell u_\ell}{D_p^2} + 1.75\,\frac{1-\phi}{\phi^3}\frac{\rho_\ell u_\ell^2}{D_p}.$$

In the present case it is unclear which of the Darcy or kinetic terms is the more important, which is why we use the general law (25) (though for simplicity most of the subsequent detailed calculations will be carried out using the Darcy term only). Some idea of the relative sizes of the the two terms on the right hand side of (27) may be gained, however, by considering the ratio R_d of the first to the second term. We find that

$$R_d = \frac{86\nu_\ell(1-\phi)}{u_\ell D_p},$$

where $\nu_\ell \sim 10^{-6}\mathrm{m}^2/\mathrm{s}$ is the kinematic viscosity of the liquid. R_d may thus be thought of as an inverse pore Reynolds number which includes a scale factor that reflects experimental results. To estimate R_d we need to estimate u_ℓ and D_p: tentatively taking $u_\ell \sim 2\mathrm{m/s}$, $D_p \sim 10^{-5}\mathrm{m}$ and $\nu_\ell \sim 10^{-6}$ gives $R_d \sim 4.3$ which probably indicates that both the Darcy and kinetic terms are important. In the absence of any firm data however, we postpone further discussion of this topic and simply use (26) from now on.

2.2.2 ELASTICITY:

To allow proper consideration of the elastic forces in the problem we must first relate the elastic displacements to the felt velocity. This is easily accomplished by observing that, by definition,

$$\boldsymbol{U}_t + \boldsymbol{q}_f.\nabla\boldsymbol{U} = \boldsymbol{q}_f. \tag{28}$$

The equation (28) is not strictly a constitutive law, and to complete the specification of the problem it is necessary to state how the stress tensor in the felt depends upon the felt displacements. Traditionally, most deformable porous medium models have made the simplifying assumption that linear elasticity applies, and we shall do so here. Nevertheless, there is also some experimental evidence that suggests that the felt does not behave as a linearly elastic body, but rather is able to compress in a vertical direction without expanding *at all* in a horizontal direction. In reality, the felt is composed of a complicated juxtaposition of different nylon layers, and though it is clearly much too hard to try to model the mechanical properties of the felt in any detail, we wish to allow for the possibility that the felt may compress without expanding. We thus propose (and later evaluate) two different elasticity models:

Linear Elastic Model

When the assumption of linear elasticity is used for the felt, we simply write

$$\boldsymbol{\tau}_f = \lambda \mathrm{div}\boldsymbol{U}\boldsymbol{I} + \mu(\nabla\boldsymbol{U} + \nabla\boldsymbol{U}^T)$$

in the normal way, where λ and μ are the Lamé constants. Thus, in non-dimensional variables,

$$\boldsymbol{\tau}_f^* = \frac{\lambda}{E}\mathrm{div}^*\boldsymbol{U}^*\boldsymbol{I} + \frac{\mu}{E}(\nabla^*\boldsymbol{U}^* + \nabla^*\boldsymbol{U}^{*T}).$$

In the most general cases we expect that λ and μ may depend on γ (though in the calculations presented below, we simply assume that the Lamé constants are independent of the void fractions).

A "Rigid Felt" Elastic Model

To propose an elastic model that mimics some of the observed experimental behavior of the felt we assume that the felt is completely rigid (incompressible) in the horizontal direction, but can be compressed vertically. This is tantamount to assuming that (in dimensional variables)

$$\boldsymbol{U} = \begin{pmatrix} u_\infty t \\ W(x,z,t) \end{pmatrix}$$

and thus in non-dimensional variables $\boldsymbol{U}^* = (t^*, W^*(x^*, z^*, t^*))^T$. With this constitutive assumption, the x-component of the felt momentum equation effectively disappears and the horizontal felt velocity is known. There is a great advantage in treating the elasticity in the problem in this fashion, for the problem may now be closed by assuming that τ_{f22} is a "known" function of the felt fraction γ. Since experiments have been carried out, it is reasonable to assume that this function will be quite well established; in any case, it is clear that the functional form of τ_{f22} must be as shown in figure

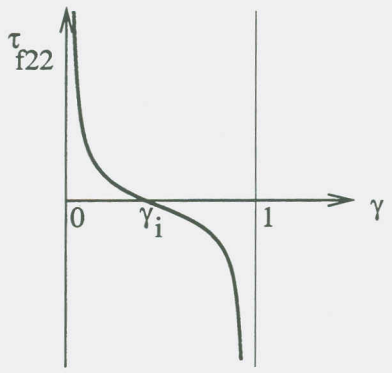

Figure 3: Functional form of relationship between τ_{f22} and γ. (Point of zero stress assumed to occur at $\gamma = \gamma_i$.)

3. It is worth pointing out again that τ_{f22} should regarded as a tension force; as shown in figure 3 infinite tension ($\tau_{f22} \to \infty$) implies zero felt fraction, whilst when the tension tends to $-\infty$ (infinite compression) the felt fraction is 1: the elastic tension in the felt is assumed to be zero when $\gamma = \gamma_i$.

We shall see later that modeling the felt elasticity in this way allows a great deal of progress to be made in closed form; it should be remembered, however, that we are essentially proposing a nonlinear theory where the elastic displacements are not small. We may anticipate that a theoretical derivation of this model involving any rigor might be very hard to carry out, and the detailed assumptions that this model is based upon are therefore a little unclear.

3 Analysis of Particular Cases - Arbitrary Geometry

Now that the model has been posed in some generality in the form of (19)–(24) and the constitutive laws for drag and elasticity discussed in section 2.2, it is possible to analyze a number of particular cases. Space does not permit a full analysis of each case; we either indicate the methodology that would need to be employed to calculate solutions, or proceed in some detail to obtain results.

3.1 Linear Elasticity - Arbitrary Geometry

When we assume that the felt deforms as a linear elastic medium, we may separate the flow into two distinct regimes, namely saturated (no air present) and unsaturated ($\beta > 0$). When $\beta > 0$, (23) gives $p = 0$ so that $\boldsymbol{D}_{\ell f} = 0$ and thus $\boldsymbol{q}_\ell = \boldsymbol{q}_f$. When $\beta = 0$, (20) and (23) vanish and it is convenient to add (22) to (24). In these two regimes the non-dimensional equations are therefore

Unsaturated:

$$\alpha_t + \nabla.(\alpha \boldsymbol{q}_\ell) = 0 \tag{29}$$

$$\beta_t + \nabla.(\beta \boldsymbol{q}_a) = 0 \tag{30}$$

$$\gamma_t + \nabla.(\gamma \boldsymbol{q}_f) = 0 \tag{31}$$

$$\boldsymbol{q}_\ell = \boldsymbol{q}_f \tag{32}$$

$$\nabla.\boldsymbol{\tau}_f = 0 \tag{33}$$

$$\boldsymbol{U}_t + (\boldsymbol{q}_f.\nabla)\boldsymbol{U} = \boldsymbol{q}_f \tag{34}$$

$$\boldsymbol{\tau}_f = \frac{\lambda}{E}(\mathrm{div}\boldsymbol{U})\boldsymbol{I} + \frac{\mu}{E}(\nabla\boldsymbol{U} + \nabla\boldsymbol{U}^T) \tag{35}$$

Saturated:

$$\begin{aligned}
\alpha_t + \nabla.(\alpha \boldsymbol{q}_\ell) &= 0 && (36)\\
\gamma_t + \nabla.(\gamma \boldsymbol{q}_f) &= 0 && (37)\\
\alpha \nabla p &= \boldsymbol{D}_{\ell f} && (38)\\
\nabla.\boldsymbol{\tau}_f &= \nabla p && (39)\\
\boldsymbol{U}_t + (\boldsymbol{q}_f.\nabla)\boldsymbol{U} &= \boldsymbol{q}_f && (40)\\
\boldsymbol{\tau}_f &= \frac{\lambda}{E}(\mathrm{div}\boldsymbol{U})\boldsymbol{I} + \frac{\mu}{E}(\nabla \boldsymbol{U} + \nabla \boldsymbol{U}^T) && (41)\\
\boldsymbol{D}_{\ell f} &= -\frac{K\alpha}{k(\alpha)}(\boldsymbol{q}_\ell - \boldsymbol{q}_f) g(Re_p, \alpha) && (42)
\end{aligned}$$

The methodology for determining the solution in each region is as follows: for unsaturated flow, we begin by solving the decoupled equations (33) to determine the felt displacements. The felt velocity $\boldsymbol{q}_f$ may then be determined by solving (34). The liquid velocity $\boldsymbol{q}_f$ is now known from (32) and the volume fraction of liquid may be found by solving (29). The equation (31) may now be solved to determine β. The only quantity that cannot be determined is $\boldsymbol{q}_a$ (equation (30) is only a scalar equation); if a detailed profile of $\boldsymbol{q}_a$ was required then the model would have to be changed slightly so that other drag terms (which we have taken to be zero) are included. It seems rather unlikely however that knowledge of $\boldsymbol{q}_a$ might ever be helpful.

Calculations continue in unsaturated regions of the flow as described above until β first becomes equal to zero. The saturated flow equations must then be solved. The simplest way to proceed in general seems to be to first add (36) to (37) and express $\boldsymbol{q}_\ell$ in terms of $\boldsymbol{q}_f$. We may then eliminate ∇p between (38) and (39) and solve the resulting equations along with (40), (41) and (42) for $\boldsymbol{q}_f$ and $\boldsymbol{U}$. For a general case however the saturated equations seem harder to solve than the unsaturated ones due to the greater degree of coupling present.

3.2 "Rigid Felt" Elasticity - Arbitrary Geometry

When the "rigid felt" elasticity model is used, the equations may once again be separated into those applying in unsaturated and saturated regions.

First, consider the unsaturated version of the equations (19)-(24). Since for unsaturated flow the air void fraction β is non-zero, we must have $\nabla p = 0$ and so from (22) we find that $\boldsymbol{D}_{\ell f} = 0$. Thus $w_\ell = w_f$ and, since we have already assumed that $u_f = 1$, it must be the case that $u_\ell = u_f = 1$. We may now add (22) and (24); this gives $\nabla.\boldsymbol{\tau} = 0$. The first of these two equations (as discussed above) is degenerate, whilst the second simply gives $(\tau_{f22})_z = 0$. Since τ is assumed to be a known non-trivial function of γ, it must be true that $(\alpha + \beta)_z = 0$.

Now suppose that the flow is saturated so that $\beta = 0$. Equations (20) and (23) vanish, and adding (22) and (24) shows that $-\nabla p + \nabla.\tau_{f22} = 0$. Again, the first component of this equation may be discarded. The equations for the rigid felt elasticity model are therefore

Unsaturated:

$$\begin{aligned}
\alpha_t + \nabla.(\alpha \boldsymbol{q}_\ell) &= 0 && (43)\\
\beta_t + \nabla.(\beta \boldsymbol{q}_a) &= 0 && (44)\\
\gamma_t + \nabla.(\gamma \boldsymbol{q}_f) &= 0 && (45)\\
(\alpha + \beta)_z &= 0 && (46)
\end{aligned}$$

$$\nabla p = 0, \quad \beta > 0 \tag{47}$$
$$u_\ell = u_f = 1, \qquad w_\ell = w_f \tag{48}$$

Saturated:

$$\alpha_t + \nabla.(\alpha \boldsymbol{q}_\ell) = 0 \tag{49}$$
$$\gamma_t + \nabla.(\gamma \boldsymbol{q}_f) = 0 \tag{50}$$
$$\beta = 0 \tag{51}$$
$$-\alpha \nabla p + \boldsymbol{D}_{\ell f} = 0 \tag{52}$$
$$-p_z + (\tau_{f22})_z = 0 \tag{53}$$

The general methodology of solution is now as follows: for unsaturated regions, we exploit that fact that $(\alpha + \beta)_z = 0$ and $w_f = w_\ell$ to solve for w_f. It is then normally possible to obtain a single hyperbolic equation for one of the void fractions. For saturated flow (53) may be integrated to determine p and thus $\boldsymbol{D}_{\ell f}$ from (52). It is then sometimes possible to eliminate one of the void fractions in favor of the other.

4 Linear Elasticity - Thin Layer Geometry

We shall now examine the linearly elastic problem in a thin layer, assuming that the flow is both steady and completely saturated. We rescale the non-dimensional variables in equations (36)–(42) according to $z = \epsilon \bar{z}$, $U = t + \epsilon^2 \bar{U}$, $W = \epsilon \bar{W}$, $u_\ell = 1 + \epsilon^2 \bar{u}_\ell$, $w_\ell = \epsilon \bar{w}_\ell$, $u_f = 1 + \epsilon^2 \bar{u}_f$, $w_f = \epsilon \bar{w}_f$ and $p = \Gamma p$ where $\epsilon = h_0/L$ and

$$\Gamma = \frac{L \mu_\ell u_\infty \epsilon^2}{E a^2} = \epsilon^2 K.$$

It is worth pointing out that this is *not* the standard "lubrication theory" limit since perturbations in the horizontal velocities and displacements are *smaller* than those in the z-direction.

Dropping the bars, we find that to leading order the equations that must be solved are

$$\alpha_x + (\alpha w_\ell)_z = 0 \tag{54}$$
$$\gamma_x + (\gamma w_f)_z = 0 \tag{55}$$
$$p_x = -c_D(\alpha)(u_\ell - u_f) \tag{56}$$
$$p_z = -c_D(\alpha)(w_\ell - w_f) \tag{57}$$
$$U_x + w_f U_z = u_f \tag{58}$$
$$W_x + w_f W_z = w_f \tag{59}$$
$$\Gamma p_x = \frac{(\lambda + \mu)}{E} W_{zx} + \frac{\mu}{E} U_{zz} \tag{60}$$
$$\Gamma p_z = \frac{(\lambda + 2\mu)}{E} W_{zz} \tag{61}$$

where $c_D(\alpha) = g(Re_p, \alpha)/k(\alpha)$.

Using the values $L \sim 0.02$m, $\mu_\ell \sim 10^{-3}$kg/m/s, $u_\infty \sim 20$m/s, $\epsilon \sim 10^{-1}$, $E \sim 10^7$Pa and $a \sim 10^{-5}$m, we find that

$$\Gamma \sim 4 \times 10^{-3}.$$

When we pass to the limit $\Gamma \to 0$, (and additionally assume that the Lamé constants λ and μ and the drag coefficient c_D are constants that are independent of α) the equations (54)–(61) are

particularly simple, and may be solved in closed form. Since in the thin layer limit only the distance between the two rollers concerns us, we assume for simplicity that the flow takes place in the region $-1 \leq x \leq 1$, $0 \leq z \leq h(x)$ where $h(x)$ is prescribed. (For simplicity we set $\phi = h(-1)$.) As far as boundary conditions are concerned, on $z = 0$ we have $U = W = 0$ as there can be no elastic displacement on the bottom surface. For analysis of a simple case, we also assume that $p = 0$ on $z = 0$, which is tantamount to assuming that there is no resistance to water flow on the bottom roller. At $x = -1$, where the squeezing process commences, we assume that $W = 0$, $\gamma = \gamma_0(z)$ where $\gamma_0(z)$ is prescribed and

$$\int_0^\phi U dz = 0,$$

the last condition arising from the usual thin layer flow stricture which dictates that that we may prescribe only the integral of U to be zero rather than U itself. On the top roller $z = h(x)$, we may apply the conditions that there is no flow of liquid normal to the roller and the felt velocity must be the same as the roller velocity. Thus (in dimensional variables) we have

$$\boldsymbol{q}_\ell.\hat{\boldsymbol{n}} = 0, \qquad \boldsymbol{q}_f.\hat{\boldsymbol{n}} = \boldsymbol{q}_R.\hat{\boldsymbol{n}} \qquad \text{and} \qquad \boldsymbol{q}_f.\hat{\boldsymbol{t}} = \boldsymbol{q}_R.\hat{\boldsymbol{t}},$$

where $\hat{\boldsymbol{n}}$ is the unit outward normal to the flow region, $\hat{\boldsymbol{t}}$ is the unit tangent and $\boldsymbol{q}_R$ is the roller velocity. Since (in non-dimensional scaled variables) $\hat{\boldsymbol{n}}$ and $\hat{\boldsymbol{t}}$ are given by

$$\hat{\boldsymbol{n}} = \frac{1}{\sqrt{1+\epsilon^2 h_x^2}} \begin{pmatrix} -\epsilon h_x \\ 1 \end{pmatrix}, \quad \hat{\boldsymbol{t}} = \frac{1}{\sqrt{1+\epsilon^2 h_x^2}} \begin{pmatrix} 1 \\ \epsilon h_x \end{pmatrix}$$

we find that, to leading order on $z = h(x)$ we have

$$w_f = w_\ell = h', \qquad u_f + \frac{h_x^2}{2} = 0.$$

The solution to (54)–(61) is then easily seen to be given by

$$w_f = \frac{zA'}{1-A}, \qquad W = Az, \qquad A = 1 - \frac{\phi}{h},$$

$$\gamma = \frac{\phi}{h}\gamma_0\left(\frac{z\phi}{h}\right), \qquad \alpha = 1-\gamma, \qquad w_\ell = \frac{h' - \gamma w_f}{\alpha}, \qquad p = c_D \int_0^z \frac{w_f - h'}{\alpha} dz.$$

The horizontal displacement U is given by

$$U = -A'\left(\frac{\lambda+\mu}{\mu}\right)\frac{z^2}{2} + Bz,$$

where the function B is defined by

$$B = \frac{1}{h}\int^x \left[\left(\frac{\lambda+\mu}{\mu}\right)\left[\frac{A''h^2}{2} + A'hh'\right] - \frac{h'^2}{2}\right] dx + \frac{C}{h}$$

and the constant C is chosen so that

$$\int_0^\phi U(-1,z)dz = 0.$$

Finally, we have

$$u_f = U_x + w_f U_z, \qquad u_\ell = u_f - \frac{p_x}{c_D}.$$

Evidently many illustrative cases may be considered; we examine only the case where $h(x) = 1 + x^2$ (a "locally circular" roller) and γ_0 is taken to be a constant. Using the above solution now gives

$$w_f = \frac{2zx}{1+x^2}, \quad W = \frac{z(x^2-1)}{1+x^2}, \quad \gamma = \frac{2\gamma_0}{1+x^2}, \quad \alpha = \frac{1+x^2-2\gamma_0}{1+x^2},$$

$$p = \frac{c_D z x (z-2-2x^2)}{1+x^2-2\gamma_0}, \quad w_\ell = \frac{2x((1+x^2)^2-2z\gamma_0)}{(1+x^2)(1+x^2-2\gamma_0)}$$

$$u_f = \frac{2z((\lambda+\mu)(1-z)+\lambda x^2-\mu x^4)}{\mu(1+x^2)^2},$$

$$U = \frac{2z((1+x^2)(\lambda-\mu x^3)+3x(\lambda+\mu)(x^2+1-z))}{3\mu(1+x^2)^2},$$

$$u_\ell = \frac{\gamma_0^2(8(\lambda+\mu)(1-z)+8x^2(\lambda-\mu x^2))}{\mu(1+x^2-2\gamma_0)^2(1+x^2)^2} -$$

$$\frac{2\gamma_0(1+x^2)[4\lambda(1+x^2-z)+\mu(2x^4-zx^2+8x^2-5z+6)]}{\mu(1+x^2-2\gamma_0)^2(1+x^2)^2} +$$

$$\frac{(1+x^2)^2[2\lambda(1+x^2-z)+\mu(4+4x^2+zx^2-3z)]}{\mu(1+x^2-2\gamma_0)^2(1+x^2)^2}.$$

Figure 4 shows plots of various components of the solution derived above; values of $c_D = 1$ and $\gamma_0 = 4/10$ were used. In figure 4(a) pressure contours are shown for the values $p = 3..(-0.5)..-3$. As expected, the pressure is highest at the entry to the nip region and lowest at the exit. Pressure plots are shown in figure 4(b). These display the expected behavior in that for fixed z the pressure decreases as the nip point is passed. In figure 4(c) contours of the liquid velocity w_ℓ (for the values $w_\ell = 3..(-0.5)..-3$) are shown. Water is expelled from the felt in $x < 0$, whilst for $x > 0$ the felt sucks water back in again. Finally, figure 4(d) shows plots of the felt velocity w_f for three values of z. As we expect, large values of z give rise to larger felt velocities.

A number of interesting points arise from the solution given above:

- We note that if γ_0 exceeds $1/2$ some components of the solution inevitably possess singularities; this is to be expected because the "compression ratio" (the ratio of the minimum channel width to the maximum channel width) in this example is $1/2$. Since we impose $W = 0$ on $z = 0$ it is not possible to compress the felt beyond the point where it completely fills the channel.
- The elasticity constants λ and μ only enter explicitly into U, u_f and u_ℓ. This is to be expected as effect of including elasticity is to modify the smaller order (viz horizontal) speeds.
- If the initial void fraction is assumed to be uniform across the felt, then the void fractions remain uniform throughout compression and are functions of x alone.
- The drag coefficient c_D enters only into the pressure; this is evident as the drag may obviously be scaled out of this leading-order thin layer problem by simply scaling the pressure.
- The pressure cannot be made to satisfy $p = 0$ at $x = \pm 1$.

The last item discussed above is not unexpected; in the limit as $\Gamma \to 0$ a p-derivative is lost in each of (60) and (61) and we might therefore anticipate that the pressure exhibits boundary layer behavior near to the edges of the nip press region. This may be confirmed by rescaling (54)–(61)

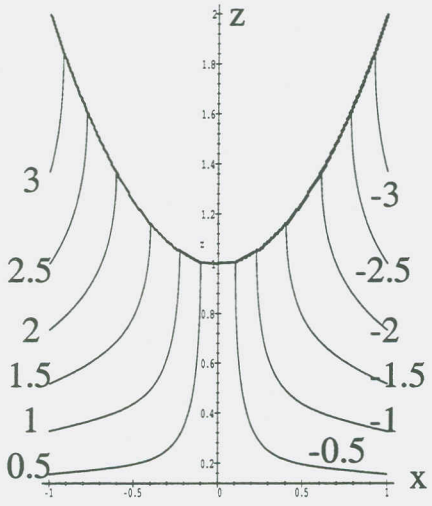

4a: pressure contours

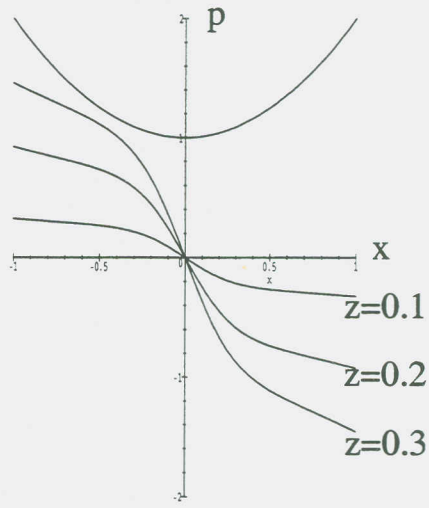

4b: pressure

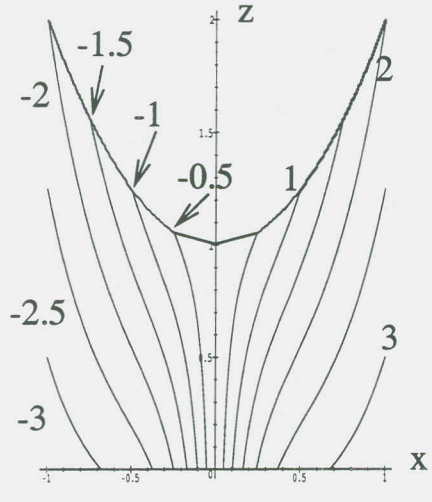

4c: contours of w_l

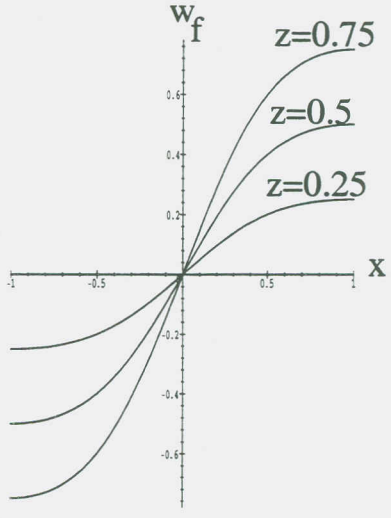

4d: w_f

Figure 4: Solution components for saturated linear elasticity model

according to $x = -1+\Gamma\tilde{x}$, $u_f = (1/\Gamma)\tilde{u}_f$, $u_\ell = (1/\Gamma)\tilde{u}_\ell$ and $W = \Gamma\tilde{W}$. The boundary layer equations then become

$$\begin{aligned}
\alpha &= \alpha(z) && (62)\\
\gamma &= \gamma(z) && (63)\\
p_{\tilde{x}} &= -c_D(\tilde{u}_\ell - \tilde{u}_f) && (64)\\
p_z &= -c_D(w_\ell - w_f) && (65)\\
U_{\tilde{x}} &= \tilde{u}_f && (66)\\
\tilde{W}_{\tilde{x}} &= w_f && (67)\\
p_{\tilde{x}} &= \frac{(\lambda+\mu)}{E}\tilde{W}_{z\tilde{x}} + \frac{\mu}{E}U_{zz} && (68)\\
p_z &= \frac{(\lambda+2\mu)}{E}\tilde{W}_{zz}. && (69)
\end{aligned}$$

Thence $\alpha_0 w_\ell + \gamma_0 w_f = A(\tilde{x})$ and so

$$w_\ell = \frac{A(\tilde{x}) - (1-\alpha_0)w_f}{\alpha_0}.$$

Physically, the boundary layer scalings tell us that (as we already knew from the outer solution) vertical displacements in the felt are small near the edges of the nip region. They also tell us that, to allow the pressure to "adjust", the horizontal liquid and felt velocities must be an order of magnitude greater than they are under most of the roller.

The boundary layer problem (62)–(69) may in fact be solved for general $h(x)$: here we simply determine the solution for the example that we examined previously where $h(x) = 1 + x^2$. In this case we have $h_x = 2x = -2 + O(\Gamma)$. Imposing the necessary

boundary condition on the roller now gives that, to leading order in the boundary layer, $A(\tilde{x}) = -2$. Eliminating p_z between (65) and (69) now gives

$$\tilde{W}_{zz} = -\left(\frac{Ec_D}{\lambda+2\mu}\right)\left(\frac{-2-\tilde{W}_{\tilde{x}}}{\alpha_0}\right)$$

and so setting

$$\kappa = \frac{\alpha_0(\lambda+2\mu)}{Ec_D}$$

we find that $\tilde{W}$ must satisfy the parabolic boundary value problem

$$\tilde{W}_{\tilde{x}} = \kappa\tilde{W}_{zz} - 2$$

in $\tilde{x} \geq 0$, $0 \leq z \leq 2$ with boundary conditions

$$\tilde{W}(\tilde{x}, 0) = 0, \qquad \tilde{W}(0, z) = 0, \qquad \tilde{W}(2, z) = -2\tilde{x}.$$

The solution to this boundary value problem may be determined by elementary means to be

$$\tilde{W} = -\tilde{x}z + \frac{1}{\kappa}\left(-\frac{z^3}{6} + z^2 - \frac{4z}{3}\right) + \sum_{n=1}^{\infty}\frac{16}{n^3\pi^3\kappa}\exp\left(-\frac{\tilde{x}n^2\pi^2\kappa}{4}\right)\sin\left(\frac{n\pi z}{2}\right),$$

and so, since an integration of (69) gives

$$p = \frac{(\lambda+2\mu)}{E}\tilde{W}_z + Q(\tilde{x})$$

we simply have to determine $Q(\tilde{x})$ so that $p = 0$ at $\tilde{x} = 0$ and $z = 0$. Doing this, we find that in the boundary layer the pressure is given by

$$p = \frac{(\lambda + 2\mu)}{E\kappa}\left(-\frac{z^2}{2} + 2z\right) + \sum_{n=1}^{\infty} \frac{8(\lambda + 2\mu)}{\pi^2 n^2 \kappa E} \exp\left(-\frac{\tilde{x} n^2 \pi^2 \kappa}{4}\right)\left[\cos\left(\frac{n\pi z}{2}\right) - 1\right].$$

As $\tilde{x} \to \infty$ and we leave the boundary layer, we find that

$$p \to \frac{(\lambda + 2\mu)}{2E\kappa} z(4 - z)$$

which agrees exactly with the inner limit of the outer solution, confirming that matching is automatic and the pressure can be made to behave in the correct fashion. An almost identical procedure may be also carried out to ensure that $p = 0$ at $x = 1$.

4.1 Linear Elasticity, Thin Layer Geometry, "Small Elastic Advection" limit

One other limit of the linear elasticity thin layer model in which great simplifications may be made occurs when we (somewhat arbitrarily) set the nonlinear terms in (58) and (59) equal to zero. We refer to this as the "limit of small elastic advection". Obvious simplifications may now we made and it is found that W satisfies a diffusion equation. This part of the problem decouples, and once W has been determined the rest of the solution may be recovered. This particular strain of analysis is more interesting when the Ergun rather than the Darcy law is used for the drag; although we omit the details in the present study, it may be shown that now W obeys a nonlinear diffusion equation.

Evidently there is much mileage in the linear elasticity problem. It is also possible to analyze cases where the flow is not saturated everywhere and a saturation free boundary must be determined. We do not pursue any further cases using the linear elasticity submodel in this report, however.

5 "Rigid Felt" Elasticity - Thin Layer Geometry

Although the results of section 4 are instructive, there is quite a lot of experimental evidence to suggest that the felt does not, in reality, behave in a linearly elastic fashion. Therefore we now turn our attention to the previously-posed rigid felt elasticity model in the thin layer limit. We again rescale according to

$$z = \epsilon\bar{z}, h = \epsilon\bar{h}, W = \epsilon\bar{W}, p = \Gamma\bar{p}, \tau_{f22} = \Gamma\bar{\tau}_{f22},$$
$$w_\ell = \epsilon\bar{w}_\ell, w_a = \epsilon\bar{w}_a, w_f = \epsilon\bar{w}_f. \tag{70}$$

It is now necessary to consider carefully the boundary condition on the bottom roller, which we take to be at $z = 0$. (Once again, since we are examining the thin layer limit, it is merely the distance between the rollers that is important, so it is convenient to assume that the bottom roller is at $z = 0$.) Much discussion took place at the meeting concerning the prescription of realistic boundary conditions on $z = 0$. Simply putting $p = 0$ there (no resistance to flow) allows water to be sucked back into the felt after it has been expelled, and it is likely that water that enters the bottom roller is, in reality, removed very quickly from the system. Our general impression was that before the nip point is reached water was expelled, whilst after the nip point mainly air was sucked back into the felt. Some experimentation with the mathematical model also showed that, depending on the pressure boundary condition that is imposed on the bottom roller, many different free boundary problems may arise. Clearly this is a facet of the problem that would benefit from a great deal of further discussion.

5.1 "Rigid Felt" Elasticity - Thin Layer Geometry - "Simplest" Problem - Theory

As we have seen, there are many ways in which the rigid felt/thin layer model may be proposed; the main difference between each of these amounts to what we specify on the bottom roller. Perhaps the simplest of these problems may be posed as follows: we assume steady flow as usual and also that the bottom roller is flat, and that exactly at the 'nip' point (i.e. under the minimum of the top roller) the bottom of the felt is exposed to air, which can enter the pores of the felt if it is able. As far as the flow of water into the bottom roller is concerned, we assume that there is some resistance (characterized by a non-dimensional parameter λ) to flow out of the felt into the bottom roller, the (non-dimensional) boundary condition at $z = 0$ being

$$p = -\lambda w_\ell.$$

Evidently, when $\lambda \to 0$ the flow of the liquid into the bottom roller is uninhibited, whilst when $\lambda \to \infty$ no water can be squeezed out of the felt: of course, we hope that beyond the nip point the water content of the felt will be reduced. Figure 5 shows a schematic diagram of the flow that we wish to consider in detail; the regions indicated will be further explained below.

5.1.1 Flow in region 1:

We begin by considering the region $x < x_i$ that is labelled 1 in the diagram. In this region, $h = h_i$ say, and no deformation of the felt has yet taken place. The flow is unsaturated so that equations (43)-(48) apply and the pressure p is zero. We shall assume here that the vertical components of each of the phasic velocities is zero, (so that the felt does not "drip") and that the void fractions are all constant, though clearly it would possible for α and β (but not γ) to be non-trivial functions of z. The felt is assumed to be in elastic equilibrium, so that $\tau_{f22} = 0$ and thus (from figure 3) $\gamma = \gamma_i$, and the pressure, being zero at $z = 0$, is thus zero everywhere. The void fractions α_i and β_i are assumed to be given. In region 1, therefore, the solution is

$$p = 0, \quad \alpha = \alpha_i, \quad \beta = \beta_i, \quad \gamma = \gamma_i, \quad (\alpha_i + \beta_i + \gamma_i = 1)$$

$$u_\ell = u_a = u_f = 1, \quad w_\ell = w_a = w_f = 0, \quad \tau_{f22} = 0.$$

5.1.2 Flow in region 2:

In region 2 the flow is still unsaturated but now the velocities and void fractions begin to change. Scaling the variables according to (70) we still have

$$(\alpha + \beta)_{\bar{z}} = 0, \quad \nabla \bar{p} = 0, \quad u_\ell = u_f = 1, \quad \bar{w}_f = \bar{w}_\ell,$$

but now to leading order the liquid and felt void fractions respectively obey the equations

$$\begin{aligned} \alpha_x + (\alpha \bar{w}_\ell)_{\bar{z}} &= 0 \\ \gamma_x + (\gamma \bar{w}_f)_{\bar{z}} &= 0. \end{aligned} \tag{71}$$

As far as the boundary conditions are concerned, on $\bar{z} = 0$ we have $\bar{w}_\ell = \bar{w}_f = 0$, whilst on $\bar{z} = \bar{h}$ we have, to leading order, $\bar{w}_\ell = \bar{w}_f = \bar{h}_x$. First, we use (71), which, since $(\alpha + \beta)_{\bar{z}} = 0$, gives

$$(\alpha + \beta)_x = (1 - \alpha - \beta)\bar{w}_{f\bar{z}}.$$

Thus, since $\bar{w}_f = 0$ on $\bar{z} = 0$, we have

$$\bar{w}_f = \frac{\bar{z}(\alpha + \beta)_x}{1 - \alpha - \beta} = \bar{w}_\ell. \tag{72}$$

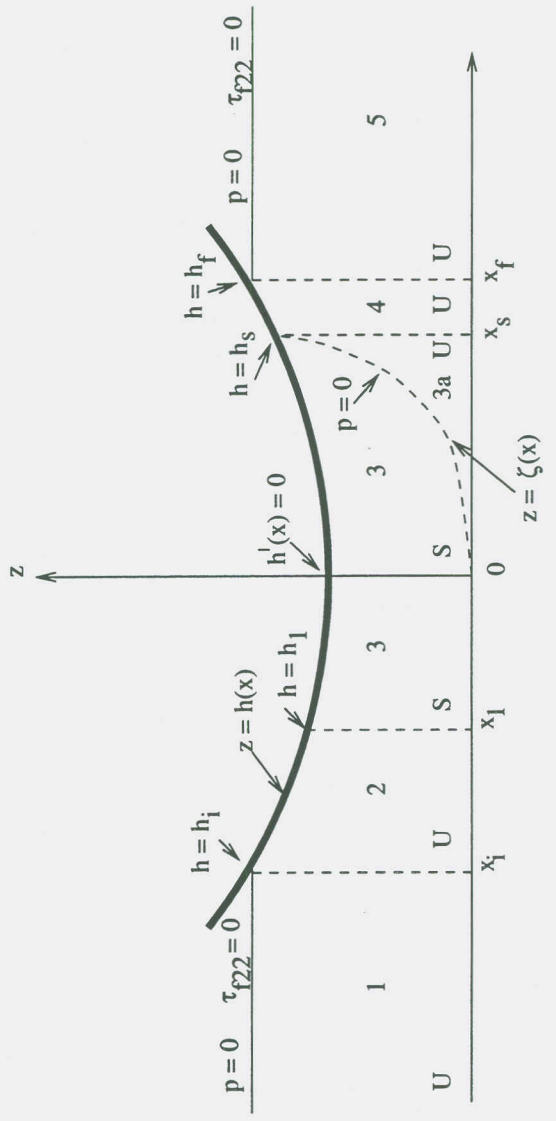

Figure 5: Schematic diagram of roll press nip for rigid felt elasticity model (U denotes unsaturated regions, S denotes saturated regions)

We may now set $\bar{z} = \bar{h}$ and $\bar{w}_f = \bar{h}'$ in (72). Integrating with respect to x, we find that

$$\bar{h}(1 - \alpha - \beta) = \text{constant},$$

and since when $\bar{h} = \bar{h}_i$ we have $\alpha = \alpha_i, \beta = \beta_i$, we find that

$$\bar{h} = \frac{\bar{h}_i(1 - \alpha_i - \beta_i)}{1 - \alpha - \beta}. \tag{73}$$

If we now use the fact that $\alpha_{\bar{z}} = 0$ (this is not immediately obvious, but if we note that α satisfies the conservation law $\alpha_x + [\alpha \bar{z} q'(x)]_{\bar{z}} = 0$ for some $q(x)$, and that $\alpha = \alpha_0 = \text{constant}$ on $x = x_i$, then it is easy to see that $\alpha = \alpha_0 \exp(-q(x) + q(x_i))$ and α must therefore be a function of x alone) then we may use that fact that $\bar{w}_\ell = \bar{w}_f$ to see that

$$\alpha_x + (\alpha \bar{w}_f)_{\bar{z}} = 0.$$

Integrating with respect to $\bar{z}$ and using fact that $\bar{w}_f = 0$ on $\bar{z} = 0$, we find that $\bar{z}\alpha_x + \alpha \bar{w}_f = 0$. Now using the boundary condition for $\bar{w}_f$ on $\bar{z} = \bar{h}$ and the initial conditions on $x = x_i$ gives

$$\alpha = \frac{\bar{h}_i \alpha_i}{\bar{h}}.$$

We may now find β from (73). We obtain

$$\beta = 1 - \frac{\bar{h}_i}{\bar{h}}(1 - \beta_i). \tag{74}$$

The solution in region 2 is now completely determined; we note that no water is lost from the felt and only air is squeezed out (this is essentially a consequence of the drag laws that were adopted). Since $\bar{w}_a = \bar{h}'$ on $\bar{z} = \bar{h}$, we have

$$\bar{w}_a = \frac{(\bar{h} - \bar{z})\beta_x}{\beta} + \bar{h}'$$

and thus the speed $\bar{w}_{a0}$ of the air lost on the lower boundary is given by

$$\bar{w}_{a0} = \frac{\bar{h}'\bar{h}}{(\bar{h} - \bar{h}_i(1 - \beta_i))}.$$

Most importantly, however, we now know where region 2 ends, for from (74) we see that when x is such that $\bar{h} = \bar{h}_i(1 - \beta_i)$ (at $x = x_1$, say), the air fraction β reaches zero and so the flow becomes saturated.

5.1.3 Flow in region 3:

As we have seen, in $x \geq x_1$ the flow is saturated and a different set of thin layer equations apply. In non-dimensional unscaled variables the general equations are

$$\begin{aligned}
\alpha_t + \nabla.(\alpha \boldsymbol{q}_\ell) &= 0 && (75)\\
\gamma_t + \nabla.(\gamma \boldsymbol{q}_f) &= 0 && (76)\\
\beta &= 0 &&\\
-\alpha \nabla p - \frac{K\alpha g}{k}(\boldsymbol{q}_\ell - \boldsymbol{q}_f) &= 0 && (77)\\
-p_z + (\tau_{f22})_z &= 0. && (78)
\end{aligned}$$

We now use the thin layer scalings (70). To leading order, (75) and (76) become

$$\begin{aligned}
\alpha_x + (\alpha \bar{w}_\ell)_{\bar{z}} &= 0 && (79)\\
(1 - \alpha)_x + ((1 - \alpha)\bar{w}_f)_{\bar{z}} &= 0 &&
\end{aligned}$$

and adding these two equations gives (since $\bar{w}_\ell = \bar{w}_f = \bar{h}'$ on $\bar{z} = \bar{h}$)

$$\alpha \bar{w}_\ell + (1-\alpha)\bar{w}_f = \bar{h}'. \tag{80}$$

The thin layer version of the $\bar{z}$-component of (77) yields

$$\bar{p}_{\bar{z}} = -c_D(\bar{w}_\ell - \bar{w}_f), \tag{81}$$

where, as before,

$$c_D = \frac{K\epsilon^2 g(Re_p, \alpha)}{\Gamma k(\alpha)} = \frac{g(Re_p, \alpha)}{k(\alpha)}$$

and once again for simplicity we assume that c_D is constant.

Next, we note that on $\bar{z} = 0$ we have $\bar{w}_f = 0$ and

$$\bar{p} = -A\bar{w}_\ell,$$

where

$$A = \frac{\lambda\epsilon}{\Gamma}.$$

Using (80) now gives that on $\bar{z} = 0$ we have

$$\bar{h}' = -\frac{\alpha\bar{p}}{A}.$$

The thin layer version of (78) may now be integrated with respect to $\bar{z}$ to yield

$$\bar{p} = \bar{\tau}_{f22} - \frac{\bar{h}'A}{\alpha} - (\bar{\tau}_{f22})\,|_{\bar{z}=0}\,.$$

Now we may use (80) and $\bar{p}_{\bar{z}} = -c_D(\bar{w}_\ell - \bar{w}_f)$ to show that

$$\bar{p}_{\bar{z}} = -\frac{c_D}{1-\alpha}(\bar{w}_\ell - \bar{h}')$$

and thus using (78), we find that

$$(\bar{\tau}_{f22})_{\bar{z}} + \frac{c_D}{1-\alpha}(\bar{w}_\ell - \bar{h}') = 0. \tag{82}$$

Finally, $\bar{w}_\ell$ may be eliminated between (79) and (82) to yield a single equation for α. The nonlinear convection-diffusion equation that applies in region 3 is therefore

$$\alpha_x + h_x\alpha_{\bar{z}} - \left[\frac{\alpha(\bar{\tau}_{f22})_{\bar{z}}(1-\alpha)}{c_D}\right]_{\bar{z}} = 0. \tag{83}$$

Two points of interest arise concerning the solution of (83) in region 3. First, the equation requires one initial and two boundary conditions. These are given respectively by

$$\alpha(x_1, \bar{z}) = \frac{\alpha_i}{1-\beta_i}$$

and

$$\alpha_{\bar{z}}(x, \bar{h}(x)) = 0, \qquad \alpha(\bar{\tau}_{f22})_{\bar{z}} = -c_D\bar{h}' \quad \text{on} \quad \bar{z} = 0.$$

(The first boundary condition may be obtained by noting that $\bar{w}_\ell = \bar{h}'$ on $\bar{z} = \bar{h}$ and thus from (82) we have $(\bar{\tau}_{f22})_{\bar{z}} = 0$ which is only possible in general if $\alpha_{\bar{z}} = 0$; to derive the second we note that $\bar{w}_f = 0$ on $\bar{z} = 0$ and so, from (80), we have $\alpha\bar{w}_\ell = \bar{h}'$ which may be combined with (82).)

Second, we note that, unlike regions 1 and 2, we do not know where region 3 ends and it is not clear how far into $x > 0$ (83) should be solved. Since in region 3 we have

$$\bar{p} = \bar{\tau}_{f22} - \frac{\bar{h}'A}{\alpha} - (\bar{\tau}_{f22})\,|_{\bar{z}=0}$$

we know that $\bar{p}$ reaches zero on $\bar{z} = 0$ when $\bar{h}' = 0$, i.e. at the "nip". Since for $x < 0$ the pressure $\bar{p}$ is evidently positive, a free boundary on which $\bar{p} = 0$ thus extends into $x > 0$ as shown in figure 5. Although this free boundary (which we shall denote in non-dimensional scaled variables by $\bar{z} = \bar{\zeta}(x)$) has yet to be determined, we know that on it $\bar{p} = 0$, and also that $\bar{w}_\ell$, $\bar{w}_f$ and α are continuous across it into region 3a.

5.1.4 Flow in region 3a:

In region 3a the flow is once again unsaturated, since for $x > 0$ air is sucked into region 3a from the bottom boundary $\bar{z} = 0$. We note first that, by (46),

$$(\alpha + \beta)_{\bar{z}} = 0$$

and thus the felt fraction, given by

$$\gamma(x) = 1 - \alpha - \beta,$$

is a function of x alone. As usual for unsaturated flow, we also have $\bar{w}_f = \bar{w}_\ell$, and the thin layer version of the felt conservation of mass equation is

$$\gamma_x + \gamma(\bar{w}_f)_{\bar{z}} = 0$$

with $\bar{w}_f = 0$ on $\bar{z} = 0$. From this we see that

$$\bar{w}_f = \bar{w}_\ell = -\frac{\bar{z}\gamma'(x)}{\gamma(x)}.$$

Conservation of mass for the liquid phase now gives

$$\alpha_x + (\alpha\bar{w}_\ell)_{\bar{z}} = 0$$

so that

$$\alpha_x = \frac{\gamma'(x)}{\gamma(x)}(\bar{z}\alpha)_{\bar{z}},$$

and thus

$$\alpha = \frac{1}{\bar{z}} f\left(\frac{\bar{z}}{\gamma(x)}\right),$$

where the function f is, as yet, unknown. However, since on the boundary $\bar{z} = \bar{\zeta}(x)$ of the saturated region we have $\beta = 0$ and therefore $\alpha = 1 - \gamma(x)$, we see that f is defined implicitly by

$$(1 - \gamma(x))\bar{\zeta}(x) = f(\bar{\zeta}(x)/\gamma(x)). \tag{84}$$

We must be sure to interpret (84) in the right way: as yet no complete problem to determine $\bar{\zeta}(x)$ has been determined, and thus neither $\gamma(x)$ nor $\zeta(x)$ are available for use in (84). We may speedily repair this omission, however: since $\bar{w}_\ell$ and $\bar{w}_f$ are equal in region 3a and continuous across $\bar{z} = \bar{\zeta}(x)$ it must be the case that $\bar{w}_\ell = \bar{w}_f$ on $\bar{z} = \bar{\zeta}(x)$. Thus, from (81), $\bar{p}_{\bar{z}} = 0$ here, and so, from (78), $(\bar{\tau}_{f22})_{\bar{z}}$ is zero on the free boundary. Thus

$$\alpha_{\bar{z}}(x, \bar{\zeta}(x)) = 0.$$

Evidently one more condition is required to determine $\bar{\zeta}(x)$: from (80) we have

$$\alpha\bar{w}_\ell + (1-\alpha)\bar{w}_f = \bar{h}',$$

and so since $\bar{w}_\ell = \bar{w}_f$ on $\bar{z} = \bar{\zeta}(x)$, it must be the case that

$$\bar{w}_\ell = \bar{w}_f = \bar{h}' \quad \text{on } \bar{z} = \bar{\zeta}(x). \tag{85}$$

In the unsaturated region 3a we have already noted that

$$\bar{w}_\ell = -\frac{\bar{z}\gamma'(x)}{\gamma(x)} \tag{86}$$

and so, combining (85) and (86) we find that, on the free boundary,

$$\bar{h}_x = -\frac{\bar{\zeta}\gamma'(x)}{\gamma(x)}.$$

Since $\beta = 0$ on the free boundary we have

$$(1-\alpha)\bar{h}' = \bar{\zeta}(\alpha_x + \bar{\zeta}'\alpha_{\bar{z}}).$$

As we have already seen, $\alpha_{\bar{z}} = 0$ when $\bar{z} = \bar{\zeta}(x)$. The final condition that determines the free boundary is thus

$$(1-\alpha)\bar{h}' = \bar{\zeta}\alpha_x.$$

We may now summarize: In region 3 we solve the well–posed problem

$$\alpha_x + h_x\alpha_{\bar{z}} - \left[\frac{\alpha(\bar{\tau}_{f22})_{\bar{z}}(1-\alpha)}{c_D}\right]_{\bar{z}} = 0$$

subject to

$$\alpha(x_1, \bar{z}) = \frac{\alpha_i}{1-\beta_i}, \qquad \alpha_{\bar{z}}(x, \bar{h}(x)) = 0,$$

$$\alpha(\bar{\tau}_{f22})_{\bar{z}} = -c_D\bar{h}' \quad \text{on } \bar{z} = 0$$

and

$$\alpha_{\bar{z}}(x, \bar{\zeta}(x)) = 0, \qquad (1-\alpha(x, \bar{\zeta}(x)))\bar{h}' = \bar{\zeta}\alpha_x(x, \bar{\zeta}(x))$$

to determine α and $\bar{\zeta}(x)$. This yields $\gamma(x)$, and, with $\bar{\zeta}(x)$ known, (84) may now be used to determine f and thus the complete solution in region 3a. It is worth pointing out that to determine the solution in region 3a, it is of course necessary that (84) possesses a unique solution. Although it seems at least plausible that this may be the case, there seems to be no *a priori* guarantee that this state of affairs does indeed prevail. Clearly more work is required on this aspect of the problem.

5.1.5 Flow in region 4:

The solution in region 3a is valid only until the free boundary hits the top roller. Let us assume that this happens at $x = x_s$, so that $\bar{\zeta}(x_s) = \bar{h}(x_s)$, and that at this point $\alpha = \alpha_s(\bar{z})$. Region 4 is unsaturated, and its only role is to allow air to re-enter the gaps that have been left by the water that has been squeezed out. The thin layer versions of (43)–(48) apply. From (46) we have

$$\gamma(x) = 1 - \alpha - \beta$$

and so the thin layer mass conservation equations give

$$\bar{w}_\ell = \bar{w}_f = -\frac{\bar{z}\gamma'(x)}{\gamma(x)} \tag{87}$$

in the same way that they did in region 3a. As before, since $\bar{w}_f = \bar{h}'$ on $\bar{z} = \bar{h}$, we find from (87) that $\gamma\bar{h}$ is constant. Region 4 ends at the point where the felt returns to its original unstressed condition and hence $\gamma = \gamma_i$ and $\tau_{f22} = 0$. Therefore

$$\gamma = \frac{\bar{h}_f(1 - \alpha_i - \beta_i)}{\bar{h}},$$

where $\bar{h}_f$ is the final total felt thickness, which in this case is simply $\bar{h}_i$. Conservation of mass for the liquid now yields the hyperbolic equation

$$\alpha_x - \left(\frac{\bar{z}\gamma'(x)\alpha}{\gamma(x)}\right)_{\bar{z}} = 0.$$

which may be solved (subject to the boundary condition that $\alpha = \alpha_s(\bar{z})$ at $x = x_s$) to give

$$\alpha = \frac{\bar{h}(x_s)}{\bar{h}(x)}\alpha_s\left(\frac{\bar{z}\bar{h}(x_s)}{\bar{h}(x)}\right). \tag{88}$$

5.1.6 Flow in region 5:

In region 5 the flow is again unsaturated and no air or water either leaves or enters the felt, which has returned to an equilibrium state. We have $\bar{h} = \bar{h}_i$ and we may read off α_o and β_o, the respective outgoing liquid and air void fractions. We find that

$$\alpha_o = \frac{\bar{h}(x_s)}{\bar{h}_i}\alpha_s\left(\frac{\bar{z}\bar{h}(x_s)}{\bar{h}_i}\right)$$

and

$$\beta_o = \alpha_i + \beta_i - \frac{\bar{h}(x_s)}{\bar{h}_i}\alpha_s\left(\frac{\bar{z}\bar{h}(x_s)}{\bar{h}_i}\right).$$

We also have $p = 0$, $u_\ell = u_a = u_f = 1$ and $\bar{w}_\ell = \bar{w}_a = \bar{w}_f = 0$. In this case, the felt returns to an unstressed state after its passage through the roller, and thus $\bar{h}_f = \bar{h}_i$ and once again $\tau_{f22} = 0$ and $\gamma = \gamma_i$ as per figure 3. By considering examples where the felt entered the roller with a non-zero stress, it would be possible to examines cases where the final and initial total felt thicknesses were not the same.

5.2 "Rigid Felt" Elasticity - Thin Layer Geometry - "Simplest" Problem - Example

We now discuss numerical methods and example calculations based on the theory detailed in section 5.1. The aim in this discussion is to first outline numerical methods designed to solve the various equations without making specific choices for the various parameters involved, such as the roller shape and elastic properties of the felt. In this way, the numerical method may be used to perform "numerical experiments" for a wide range of choices for the parameters within the theory. For the purpose of illustration, we will use the numerical methods for an example calculation assuming some simple choices for the various parameters involved.

5.2.1 Numerical methods

A numerical method of solution is needed to solve the convection-diffusion equation for α in region 3 and to find the saturation boundary, $\bar{z} = \bar{\zeta}(x)$, that separates regions 3 and 3a. Explicit formulas for α are available for the other regions, although for regions 3a, 4, and 5 the formulas rely on the numerical solution found in region 3. Once α is known, then other quantities such as the pressure p, the fractions β and γ, or the vertical velocities $\bar{w}_\ell$ and $\bar{w}_f$ can be worked out as well.

We begin with a discussion of the numerical treatment of the equations for region 3. In this region, α evolves according to the convection-diffusion equation given in (83) for $x > x_1$. An initial condition is given at $x = x_1$ and boundary condition are given on $\bar{z} = 0$ and $\bar{z} = \bar{h}(x)$ for $x_1 < x < 0$ and on $\bar{z} = \bar{\zeta}(x)$ and $\bar{z} = \bar{h}(x)$ for $0 < x < x_s$. Because the boundary conditions are given on curves, it is convenient to use the change of variable

$$\bar{z} = \bar{b}(x) + y(\bar{h}(x) - \bar{b}(x))$$

so that $\bar{z} \in [\bar{b}(x), \bar{h}(x)]$ becomes the fixed interval $y \in [0, 1]$. For our boundary-value problem, $\bar{b}(x)$ is taken to be 0 for $x_1 < x < 0$ and $\bar{\zeta}(x)$ for $0 < x < x_s$. In terms of the independent variables (x, y), the governing equation becomes

$$\alpha_x + v(x,y)\alpha_y = \frac{1}{(\bar{h}-\bar{b})^2}\left[\frac{\alpha(1-\alpha)(\bar{\tau}_{f22})_y}{c_D}\right]_y, \tag{89}$$

where $\bar{\tau}_{f22} = \bar{\tau}_{f22}(1-\alpha)$ and $c_D = c_D(\alpha)$, and

$$v(x,y) = (1-y)\frac{\bar{h}'(x) - \bar{b}'(x)}{\bar{h}(x) - \bar{b}(x)}.$$

The initial condition

$$\alpha = \frac{\alpha_i}{1-\beta_i} \qquad \text{on } x = x_1,$$

is unchanged, while the boundary conditions become

$$\alpha(\bar{\tau}_{f22})_y = -c_D\bar{h}\bar{h}' \qquad \text{on } y = 0 \text{ for } x_1 < x < 0$$

or

$$\left.\begin{aligned} \alpha_y &= 0 \\ (1-\alpha)\bar{h}' &= \bar{\zeta}\alpha_x \end{aligned}\right\} \qquad \text{on } y = 0 \text{ for } 0 < x < x_s$$

and $\alpha_y = 0$ on $y = 1$ for both intervals of x.

Let us first consider a numerical formulation of the problem for $x_1 < x < 0$. For the interval $y \in [0, 1]$ we use a uniform grid

$$y_j = (j - \tfrac{1}{2})\Delta y, \qquad \Delta y = 1/n, \qquad j = 0, 1, \ldots, n+1$$

for a chosen integer n and let $\alpha_j(x)$ approximate the exact solution on the grid. A cell-centered grid is used to facilitate the difference approximations of derivatives at the boundaries. Using central differencing for the diffusive term and upwind differencing ($v < 0$) for the convective term, (89) (with $\bar{b} = 0$) becomes

$$\frac{d}{dx}\alpha_j + v(x,y_j)\frac{\delta_+\alpha_j}{\Delta y} = \frac{\delta_+}{(\bar{h}\Delta y)^2}\left[\frac{\alpha_{j-1/2}(1-\alpha_{j-1/2})\delta_-\bar{\tau}_{f22}(1-\alpha_j)}{c_D(\alpha_{j-1/2})}\right] \tag{90}$$

for $j = 1, 2, \ldots, n$, where

$$\alpha_{j-1/2} = \tfrac{1}{2}(\alpha_j + \alpha_{j-1})$$

and δ_+ and δ_- are forward and backward difference operators, respectively, defined by

$$\delta_+\alpha_j = \alpha_{j+1} - \alpha_j \qquad \text{and} \qquad \delta_-\alpha_j = \alpha_j - \alpha_{j-1}.$$

The boundary conditions become

$$\alpha_{1/2}\delta_-\bar{\tau}_{f22}(1-\alpha_1) = -\Delta y c_D(\alpha_{1/2})\bar{h}\bar{h}' \qquad \text{and} \qquad \delta_+\alpha_n = 0.$$

We may regard these difference equations as a system of ordinary differential equations (ODEs) which take the form

$$\frac{d}{dx}\mathbf{a} + C(x, \mathbf{a}) = D(x, \mathbf{a}),$$

where $\mathbf{a} = (\alpha_1, \ldots, \alpha_n)^T$ and C and D denote the contributions from the convective and diffusive terms in (90), respectively. A first-order integration of these ODEs is

$$\frac{\mathbf{a}(x + \Delta x) - \mathbf{a}(x)}{\Delta x} + C(x, \mathbf{a}(x)) = D(x + \Delta x, \mathbf{a}(x + \Delta x)), \tag{91}$$

where $\mathbf{a}(x_1)$ is given by the initial conditions and the "time step" Δx is chosen such that

$$\Delta x \leq \Delta y \max_{1 \leq j \leq n} |v(x, y_j)| = \frac{\Delta y(-\bar{h}')}{\bar{h}}$$

for stability. The stability constraint is the usual CFL condition as given by the upwind differencing of the convective terms. The diffusive terms are handled implicitly in (91) and give no constraint on the choice of Δx. Newton's method can be used to solve the nonlinear algebraic equations in (91) in order to advance $\mathbf{a}$ from x to $x + \Delta x$.

The numerical formulation of the problem for $0 < x < x_s$ is similar to that for $x_1 < x < 0$ but must now include a numerical treatment of the saturation boundary $\bar{z} = \bar{\zeta}(x)$. For this interval of x, we take $\bar{b} = \bar{\zeta}(x)$ in (89) and use the finite difference formulation

$$\frac{d}{dx}\alpha_j + v(x, y_j)\frac{\delta_+ \alpha_j}{\Delta y} = \frac{\delta_+}{((\bar{h} - \bar{\zeta})\Delta y)^2}\left[\frac{\alpha_{j-1/2}(1 - \alpha_{j-1/2})\delta_- \bar{\tau}_{f22}(1 - \alpha_j)}{c_D(\alpha_{j-1/2})}\right] \tag{92}$$

with boundary conditions

$$\delta_- \alpha_1 = \delta_+ \alpha_n = 0 \qquad \text{and} \qquad (1 - \alpha_1)\bar{h}' = \bar{\zeta}\frac{d}{dx}\alpha_1$$

The first two of these boundary conditions along with the difference equations in (92) imply a system of ODEs that take the form

$$\frac{d}{dx}\mathbf{a} + C(x, \mathbf{a}) = D(x, \mathbf{a}),$$

where C and D now involve the unknown function $\bar{\zeta}$ (and its derivative). The third boundary condition provides an additional constraint needed to determine $\bar{\zeta}$ numerically. It is convenient to regard $\bar{\zeta}'$ as an additional unknown and solve

$$\frac{\mathbf{a}(x + \Delta x) - \mathbf{a}(x)}{\Delta x} + C(x + \Delta x, \mathbf{a}(x)) = D(x + \Delta x, \mathbf{a}(x + \Delta x)),$$

$$(1 - \alpha_1(x + \Delta x))\bar{h}'(x + \Delta x) = \bar{\zeta}(x + \Delta x)\frac{a_1(x + \Delta x) - a_1(x)}{\Delta x}$$

$$\bar{\zeta}'(x + \Delta x) = \frac{\bar{\zeta}(x + \Delta x) - \bar{\zeta}(x)}{\Delta x}$$

for $\{\mathbf{a}, \bar{\zeta}, \bar{\zeta}'\}$ at $x + \Delta x$ in terms of $\{\mathbf{a}, \bar{\zeta}\}$ at x using Newton's method. Initial values for these equations are $\mathbf{a}(0)$ and $\bar{\zeta} = 0$, where $\mathbf{a}(0)$ is the final numerical solution from the previous interval. The value for Δx is chosen to satisfy

$$\Delta x \leq \Delta y \max_{1 \leq j \leq n} |v(x, y_j)| < \Delta y \bar{\zeta}'(x)$$

for stability. Here we note that $\bar{\zeta}'$ becomes large as x tends to x_s so that Δx approaches 0. In fact the "time" stepping in x never quite reaches the exact value of x_s. Instead we assign x_s to be the value of x when $\bar{h}(x) - \bar{\zeta}(x)$ first becomes less than a chosen tolerance which is taken to be 10^{-4}.

The numerical solution in region 3 gives discrete values for $\alpha(x, \bar{z})$ along the saturation boundary $\bar{z} = \bar{\zeta}(x)$ $(y = 0)$. These values provide the necessary information needed to continue the numerical solution for $\alpha(x, \bar{z})$ into region 3a and then into regions 4 and 5. The solution in region 3a is given by (84), where the function f can be found using the discrete values of $\alpha(x, \bar{z})$ along the saturation boundary. Values for α at $x = x_s$ from the solution in region 3a specify the function α_s in (88) which gives the solution for $\alpha(x, \bar{z})$ in regions 4 and 5, respectively.

5.2.2 Example calculations

In order to illustrate the numerical methods we now make some choices for the various parameters in the system. We begin with geometry and define the upper roller shape to be $\bar{h}(x) = 1/2 + 2x^2$. (The lower roller, as usual, is assumed to be flat and situated on $\bar{z} = 0$.) For this choice, the "nip" point is $x = 0$ at which point $\bar{h} = 1/2$. Next, we consider the incoming state of the three phase air-liquid-felt system. We assume that the incoming felt has a non-dimensional scaled height of 1 and thus it first touches the upper roller at $x = x_i = -1/2$. The incoming fraction of air is taken to be $\beta_i = 1/4$ while the incoming fraction of water given by α_i will be allowed to vary to study the behavior of the system. Thus, the incoming fraction of felt is $\gamma_i = 1 - \alpha_i - \beta_i = 3/4 - \alpha_i$. Finally, we need to make assumptions regarding the flow through the felt and its elastic properties. The coefficient of drag is taken to be 1 and thus a Darcy flow through the felt is assumed. The elastic behavior of the felt is given by $\bar{\tau}_{f22}$ as shown qualitatively by the curve in figure 3. Near $\gamma = \gamma_i$ we may approximate the curve using

$$\bar{\tau}_{f22} = \sigma(\gamma_i - \gamma)$$

where σ is a positive constant. Away from γ_i we expect a deviation from this linear fit, but we will accept this approximation for all values of γ for the purposes of our illustrative example.

The uniform incoming state from region 1 provides starting information for the solution in region 2. Using the formulas in Section 5.1.2 and the choices for $\bar{h}(x)$ and the incoming fractions of air and water given above, we find

$$\alpha = \frac{\alpha_i}{1/2 + 2x^2}, \qquad \beta = 1 - \frac{3/4}{1/2 + 2x^2}, \qquad \gamma = \frac{3/4 - \alpha_i}{1/2 + 2x^2}$$

$$\bar{w}_l = \bar{w}_f = \frac{4x\bar{z}}{1/2 + 2x^2}, \qquad \bar{w}_a = \frac{8x(1 + 8x^2 - 3z + 16x^4)}{(1 + 4x^2)(-1 + 8x^2)}, \qquad p = 0$$

These formulas apply for $-1/2 \leq x \leq x_1$, where $x_1 = -1/\sqrt{8}$ is the value of x when $\beta = 0$ and the felt becomes saturated. At this point, the fractions of water and felt are

$$\alpha_1 = \frac{4\alpha_i}{3}, \qquad \gamma_1 = 1 - \frac{4\alpha_i}{3}$$

which are greater than their incoming values.

The solution in region 3 uses the numerical approach outlined previously. For a choice of α_i and σ we may solve the finite difference equations for α from $x = x_1$ to 0 and then from $x = 0$ to $x = x_s$. For the latter interval, we also obtain points on the saturation boundary $z = \bar{\zeta}(x)$.

Figure 6 shows contours of the fraction of water in the saturated region for the choice $\alpha_i = 0.5$ and $\sigma = 1.0$. The color bar to the right of the figure indicates the value for α on each contour. The interval in α between contour lines is 0.01. The black curve at the top of the figure gives the shape of the roller and the dashed curves to the left and right mark the boundaries of the saturated region, and in particular the dashed curve to the right is the free boundary $\bar{z} = \bar{\zeta}(x)$. As expected the maximum fraction of water occurs at the left saturation boundary, where $\alpha = \alpha_1 = 2/3$. For $x > x_1$, water is squeezed out of the saturated felt so that α decreases with increasing x, at least initially. Near the roller, $\bar{z} = \bar{h}(x)$, diffusion dominates and the fraction of water decreases monotonically. Near the flat surface $\bar{z} = 0$ there is a rapid decrease in α followed by a gentler increase towards

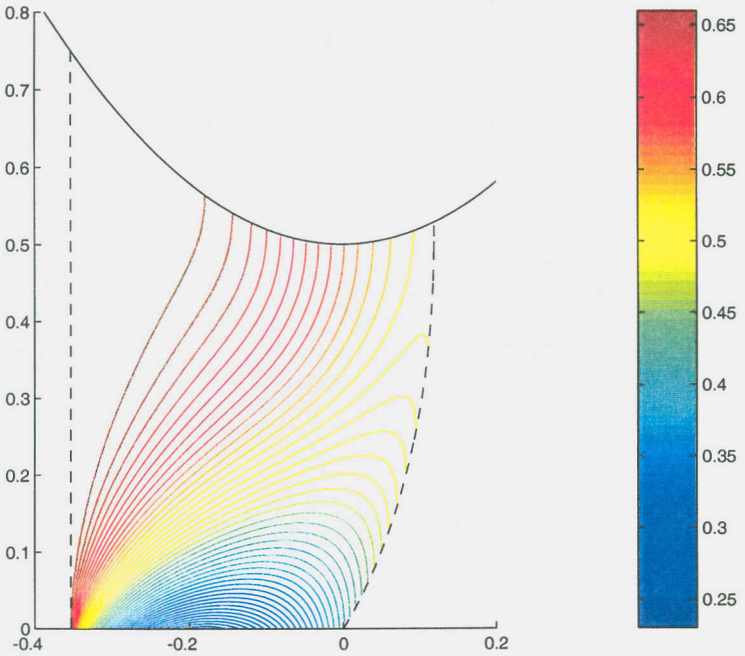

Figure 6: Water content in the saturated region for $\alpha_i = 0.5$, $\sigma = 1$.

the nip, $x = 0$. The initial decrease is in response to the geometric convergence of the roller. As the slope of the roller approaches zero near the nip, this convergence eases while diffusion tends to equilibrate the water content which causes α to increase along $\bar{z} = 0$.

Figures 7(a) and (b) give contours of α for the cases $\alpha_i = 0.5$, $\sigma = 2.0$ and $\alpha_i = 0.4$, $\sigma = 2.0$, respectively. The effect of changing the rigidity of the felt can be seen by comparing the solutions in Figures 6 and 7(a). A larger value of σ models a more rigid felt which, as seen in Figure 7(a), results in a smaller reduction in α near $\bar{z} = 0$. The effect of decreasing α_i and thus decreasing α_1 can be seen by comparing the solutions in Figures 7(a) and (b). The solution in Figure 7(b) shows a significant reduction in the minimum value of α along $\bar{z} = 0$. In fact numerical experiments with even smaller values of α_i (holding σ fixed) indicate that it is possible for this minimum to become zero implying that all water has been squeezed out of the felt at that point. The mathematical model (and numerical method) would require modification to continue the solution beyond that point.

The liquid and felt velocities, $\bar{w}_l$ and $\bar{w}_f$, respectively, can be worked out from $\alpha(x, z)$ in region 3 using (82) and (80). These velocities are shown in Figure 8 for the case $\alpha_i = 0.5$ and $\sigma = 1.0$. The liquid velocity has a minimum along $\hat{z} = 0$ where the water is leaving the felt most rapidly. The felt velocity is constrained to be zero along $\hat{z} = 0$. On the roller, both $\hat{w}_l$ and $\hat{w}_f$ are equal to $\hat{h}^(x)$ in accordance with the boundary condition there.

Once the velocities are determined, the pressure in the saturated region can be found by integrating (81) numerically from $\hat{z} = 0$ to $\hat{z} = \hat{h}(x)$ for fixed x. The boundary condition $\bar{p} = -A\bar{w}_l$ at $\hat{z} = 0$ provides the necessary information to begin the integration. Figure 9 shows the pressure for the case $\alpha_i = 0.5$, $\sigma = 1.0$, and $A = 0$. For this choice of A, the pressure is zero along $\hat{z} = 0$ which matches the value at the saturation boundaries.

Finally, we show the behavior of α for the entire interval $-1/2 \leq x \leq 1/2$ in Figure 10 for the case $\alpha_i = 0.5$ and $\sigma = 1.0$. This plot shows the behavior of the α in the unsaturated regions prior to and following the saturated region 3. Of particular interest in the plot is the fraction of liquid at $x = 1/2$, which is approximately 0.277, a value significantly less than the incoming value of 0.5.

(a)

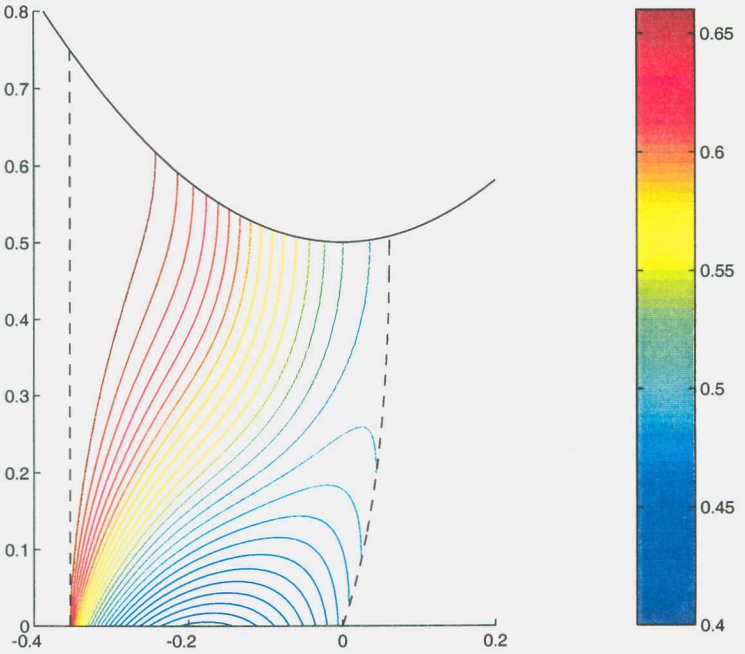

(b)

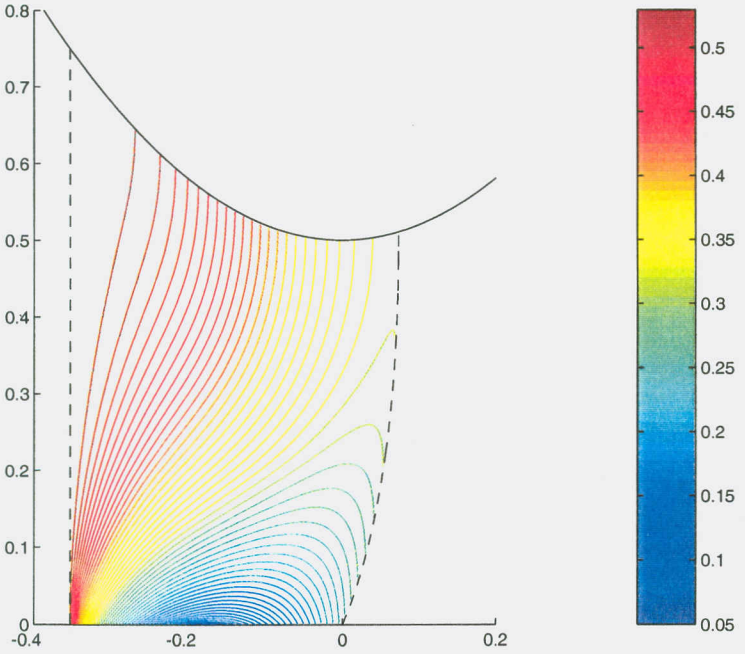

Figure 7: Water content in the saturated region for (a) $\alpha_i = 0.5$, $\sigma = 2$ and (b) $\alpha_i = 0.4$, $\sigma = 2$.

(a)

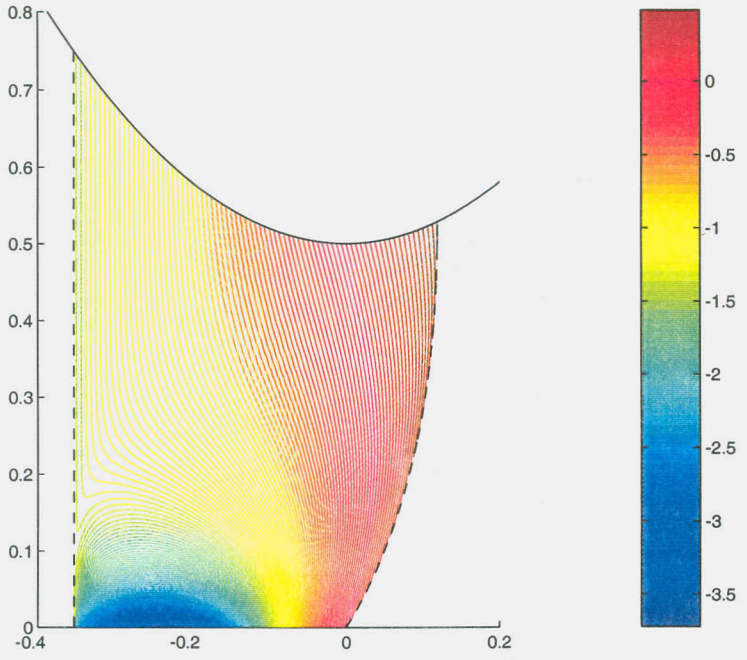

(b)

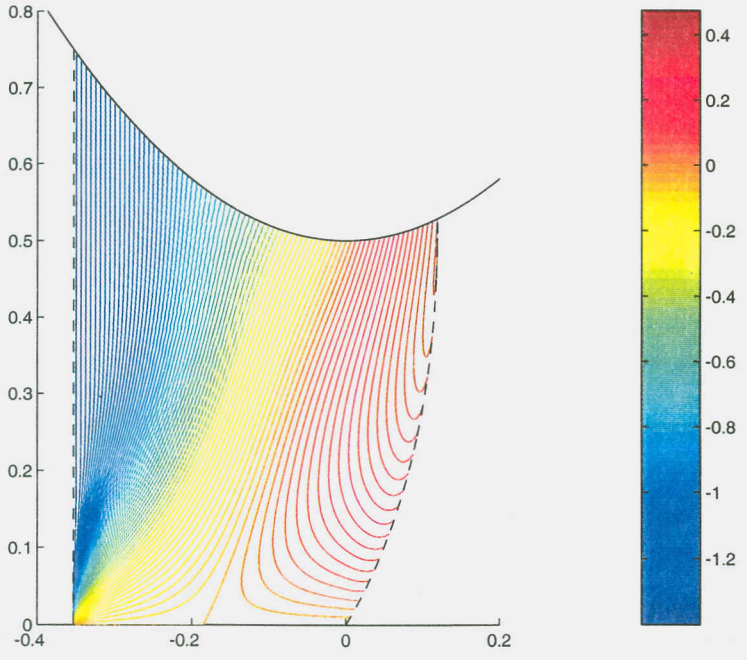

Figure 8: Vertical velocities in the saturated region for $\alpha_i = 0.5$ and $\sigma = 1$: (a) liquid velocity and (b) felt velocity

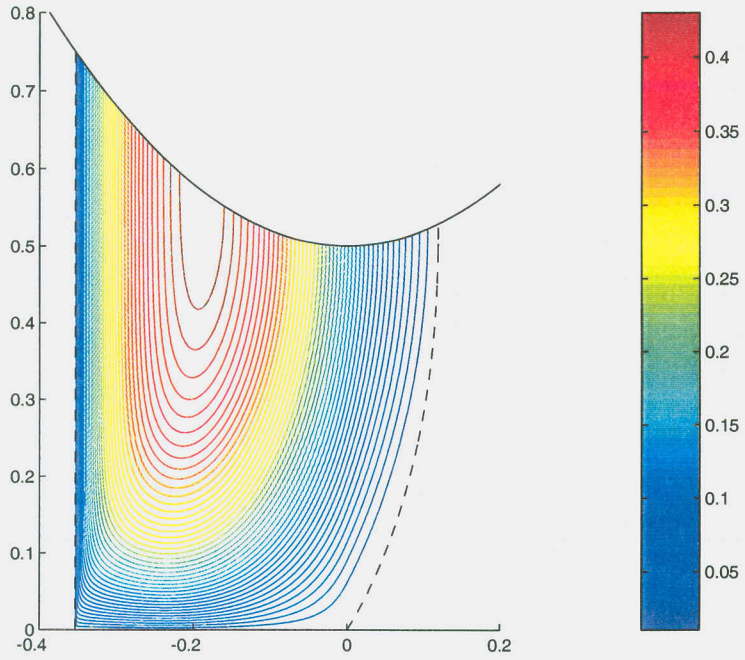

Figure 9: Pressure in the saturated region for $\alpha_i = 0.5$ and $\sigma = 1$

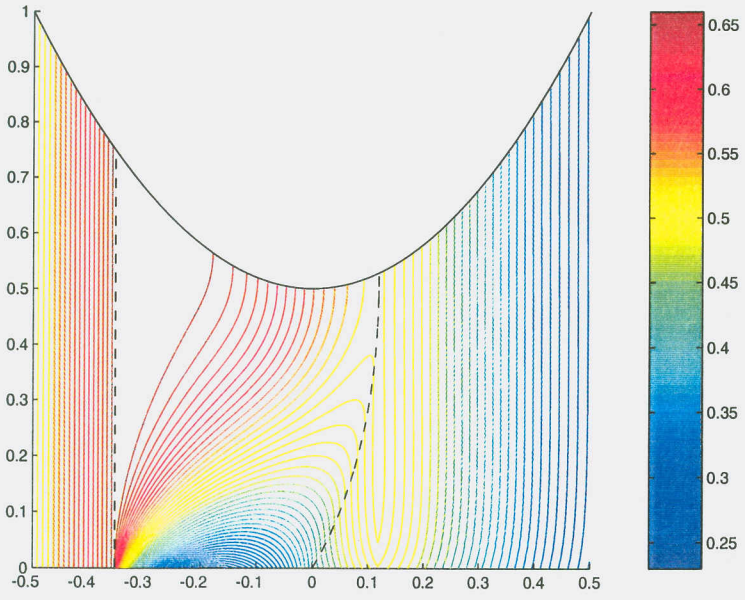

Figure 10: Water content for $\alpha_i = 0.5$ and $\sigma = 1$

6 Conclusions

We have proposed a three-phase flow model for the flow under a roll press nip. The three phases are air, water and a deformable porous medium that may be considered to be either the paper or the felt. The model has been proposed initially in some generality, before specific assumptions have been made to reduce the complexity of the working equations. We have examined a case where the felt is assumed to obey the laws of linear elasticity, and have shown that for certain restricted scenarios a complete closed-form solution is available.

As an alternative to assuming that linear elasticity applies, we also examined a case where a "rigid felt" model was proposed. In effect, this assumes that the felt is compressible only in one direction. Such behavior is suggested by experimental results. The rigid felt model produces equations that are particularly amenable to further study: if use is also made of the fact that thin layer theory applies in the gap underneath the roller, then a great deal of theoretical progress may be made: at the very least, the numerical calculations that must be performed turn out to be much simpler than those that would be required if the full system was solved. We were also able to follow the theory through for a simple example, showing the kind of water reductions that could be expected for given parameters.

Although it seems clear that we have now proposed a coherent theoretical model for the process of flow under a roll press nip, much work remains to be carried out. The following further areas of study suggest themselves:

- A careful literature survey should be carried out to determine how this model relates to previous models appearing in published literature.
- More information and comparisons should be carried out regarding the various submodels that appear within the model. Particular attention should be given to the areas of the constitutive law of the felt and the drag laws satisfied by the water and the air.
- More attention should be given to the boundary conditions that are satisfied on the bottom roller. In particular, we need to know the circumstances under which air may be sucked into the felt and how easily fluid may be removed by the bottom roller.
- More information is required concerning the state of the water-loaded felt as it approaches a roller.

References

Drew, D.A. & Wood, R.T. (1985) Overview and taxonomy of models and methods for workshop on two-phase flow fundamentals. National Bureau of Standards Report, Gaithersburg, MD.

Ergun, S. (1952) Fluid flow through packed columns, Chem. Eng. Prog. **48** 89–94.

Fitt, A.D. (1996) Mixed systems of conservation laws in industrial mathematical modelling, Surv. Math. Ind. **6** 21–53.

Reese, R.A. (Ed.) (1999) The Paper Machine Wet Press Manual (4th Edn.), TAPPI Press (Technical Association of the Pulp and Paper Industry).

Participating: (in alphabetical order)

Alistair Fitt (Faculty of Mathematical Studies, University of Southampton, Southampton SO17 1BJ UK, adf@maths.soton.ac.uk)

Bernard Fleishman (Department of Mathematical Sciences, RPI, Troy, NY 12180 USA, fleisb@rpi.edu)

Peter Howell (School of Mathematical Sciences, University of Nottingham, University Park, Nottingham NG7 2RD, UK, peter.howell@nottingham.ac.uk)

Adrienne James (Dept. of Math. Science, NJIT, University Heights, Newark, NJ 07102 USA, ajames@ylem.njit.edu)

John King (School of Mathematical Sciences, University of Nottingham, University Park, Nottingham NG7 2RD, UK, john.king@nottingham.ac.uk)

Dale Larson (10, Meriam Drive, San Rafael, CA 94903 USA)

Jeff McFadden (NIST, Gaithersburg, MD 20899 USA, mcfadden@nist.gov)

Shailesh Naire (Department of Mathematical Sciences, University of Delaware, Newark, DE 19716 USA, naire@math.udel.edu)

Colin Please (Faculty of Mathematical Studies, University of Southampton, Southampton SO17 1BJ UK, cpp@maths.soton.ac.uk)

Gilberto Schleiniger (Department of Mathematical Sciences, University of Delaware, Newark, DE 19716 USA, schleini@math.udel.edu)

Tim Schulze (Coutant Institute, NYU, 251 Mercer Street, New York, NY 10012 USA, schulze@cims.nyu.edu)

Don Schwendeman (Department of Mathematical Sciences, RPI, Troy, NY 12180 USA, schwed@rpi.edu)

John Skelton (Albany International Research Co., john_skelton@albint.com)

Burt Tilley (Dept. of Math. Science, NJIT, University Heights, Newark, NJ 07102 USA, tilley@m.njit.edu)

Report written by:

Alistair Fitt and Don Schwendeman